CHARACTERIZATION AND *IN VITRO* TOXICITY OF COPPER NANOPARTICLES (Cu-NPs) IN MURINE NEUROBLASTOMA (N2A) CELLS

THESIS

Sitao Veronica Brownheim, Capt, USAF

AFIT/GES/ENV/11-M01

DEPARTMENT OF THE AIR FORCE
AIR UNIVERSITY

AIR FORCE INSTITUTE OF TECHNOLOGY

Wright-Patterson Air Force Base, Ohio

AFIT/GES/ENV/11-M01

CHARACTERIZATION AND *IN VITRO* TOXICITY OF COPPER NANOPARTICLES (Cu-NPs) IN MURINE NEUROBLASTOMA (N2A) CELLS

THESIS

Presented to the Faculty

Department of Systems and Engineering Management

Graduate School of Engineering and Management

Air Force Institute of Technology

Air University

Air Education and Training Command

In Partial Fulfillment of the Requirements for the

Degree of Master of Science in Environmental Engineering and Science

Sitao Veronica Brownheim, BS

Capt, USAF

March 2011

AFIT/GES/ENV/11-M01

CHARACTERIZATION AND *IN VITRO* TOXICITY OF COPPER NANOPARTICLES (Cu-NPs) IN MURINE NEUROBLASTOMA (N2A) CELLS

Sitao Veronica Brownheim, BS
Capt, USAF

Approved:

//signed//	8/ March /2011
Dr. Charles A. Bleckmann (Chairman)	date
//signed//	8/ March /2011
Dr. Mark N. Goltz (Member)	date
//signed//	4/ March /2011
Dr. Amanda M. Schrand (Member) Air Force Research Laboratory	date
//signed//	4/ March /2011
Dr. Saber M. Hussain (Member) Air Force Research Laboratory	date

AFIT/GES/ENV/11-M01

Abstract

Nanomaterials, classified as materials within the 1 - 100 nanometer range, have seemingly endless applications that can be beneficial to both the military as well as to the greater society. Even with increased funding in recent years there is still a vast need for characterization data from these materials in order to quantify risks to both humans as well the environment. Nanomaterials are of great interest to the Air Force and the military because of their many applications in munitions, sensing, electronics, and life sciences including pharmaceutical drug delivery and medicine. Copper nanoparticles (Cu-NPs) have already been considered for a range of uses based on their antimicrobial properties and they are widely used in lubricants, inks and other applications that make use of their anti-microbial properties. However, the biological effects of Cu-NPs can vary based on their physicochemical properties; in particular, their oxide content and primary size. Cu-NPs can be oxidized and exist as copper oxide nanoparticles (CuO-NPs). Also, larger size Cu-NPs can exist as micron-sized copper particles (Cu-MSP). It is very important to the Air Force and especially the Bioenvironmental Engineering career field to increase the understanding of Cu-NPs and the possible health impacts from nanomaterial exposure prior to wide-spread industry and military use, particularly in occupational settings. Therefore, the purpose of this research is to thoroughly characterize the properties of three different copper samples upon suspension into aqueous solutions over time: Cu-NPs (Cu 25 nm), CuO-NPs (CuO 40 nm), and Cu-MSP (Cu 500nm). Additionally, this research seeks to observe *in vitro* effects upon murine neuroblastoma cells (N2A) by these three types of particles as well as by $CuCl_2$. Microscopy techniques indicate observable changes in oxidation for Cu-NP 25 nm and

CuO-NP 40 nm after suspension in water over long incubation. In general, agglomerations of the particles increase when dosed with the endocytosis inhibitor Dynasore. In terms of cellular viability, $CuCl_2$ is the least toxic at all concentrations. Cu-NP 25 nm is less toxic at low concentrations (< 25 μg/mL) than Cu-MSP 500 nm and CuO-NP 40 nm. At concentrations above 25 μg/mL, Cu-NP 25 nm becomes comparable in toxicity to CuO-NP 40 nm and more toxic than Cu-MSP 500 nm.

Acknowledgments

I would like to express my sincere appreciation to my faculty advisor Dr. Charles Bleckmann for his patience, mentorship, and support throughout the course of this culminating effort in my degree program. I'm thankful for Lt Col David Smith's guidance and leadership throughout my admission to AFIT as well as in the classroom. I am profoundly grateful for Dr. Amanda Schrand's proactive involvement in my research. Without her technical expertise this thesis at the Air Force Research Lab (AFRL) would not be possible. I'd like to thank Dr. Saber Hussain's willingness to collaborate with AFIT students – it is a very valuable resource to this program. I'd also like to express my gratitude to Dr. Mark Goltz, a dedicated professor who made all the difference in my studies by his enthusiasm, knowledge and love for teaching.

I am indebted to the technical guidance of many others, especially Dr. Robert Wheeler at the AFRL Materials Lab, Dr. Daniel Felker, Mr. Craig Murdock, Mr. Bradley Stacy, Ms. Christin Grabinski, Mr. Jonathan Lin, Ms. Elizabeth Maurer, Ms. Carol Garrett and others at the Biological Interactions of Nanoparticles (BIN) group at AFRL. Additionally, I'd like to thank the military members at the Applied Biotechnology branch (RHPB) for welcoming me during my short stay.

I want to express my thanks to my friends and family for their tireless support of this thesis effort. I'd also like to dedicate this thesis to my mother – from her example I am motivated on a daily basis to better myself. Last but not least, I am incredibly thankful to my wonderful husband, who keeps me grounded and always ensures that I don't lose sight of the forest for the trees.

Sitao Veronica (Gao) Brownheim

Table of Contents

Page

List of Figures

List of Tables

List of Symbols

(N2A)	Murine neuroblastoma cells
(NP)	Nanoparticles
(Cu-NP)	Copper nanoparticle
(CuO-NP)	Copper oxide nanoparticles
(Cu-MSP)	Copper micron-sized particle
(MTS)	Tetrazolium compound, 3-(4,5-dimethylthiazol-2-yl)-,5-(3-carboxymethoxyphenyl)-2-4(4-sulfophenyl) -2H-tetrazolium
(LVEM)	Low Voltage Electron Microscopy
(ESEM)	Environmental Scanning Electron Microscopy
(SEM)	Scanning Electron Microscopy
(TSCA)	Toxic Substance Control Act
(EPA)	Environmental Protection Agency
(NIOSH)	National Institute for Occupational Safety and Health
(NSF)	National Science Foundation
(AFRL)	Air Force Research Lab
(FBS)	Fetal bovine serum
(TEM)	Transmission Electron Microscopy
(DLS)	Dynamic Light Scattering
(HSI)	Hyperspectral Imaging

CHARACTERIZATION AND *IN VITRO* TOXICITY OF COPPER NANOPARTICLES (Cu-NPs) IN MURINE NEUROBLASTOMA (N2A) CELLS

I. Introduction

1.1 Background

Nanotechnology by definition means the creation and manipulation of materials at the nanoscale level (1-100 nm) and is currently "experiencing massive, world-wide investment as well as a tremendous rise in consumer products" (Schrand & Hussain, 2010). Nanotechnology is an important area of research for many reasons, including its potential to transform many industries at phenomenal speeds. Research in nanotechnologies continues to expand worldwide everyday and the National Science Foundation (NSF) estimates that nanotechnology will have a significant impact on the global economy. Specifically, the National Institute for Occupational Safety and Health (NIOSH) reports that nanotechnology will have an impact of over 1 trillion dollars and employ over 2 million workers worldwide (NIOSH, 2009).

Despite all the research and development funds pouring in, much is still unknown about potential hazards, safe handling practices, and effects on humans and the environment of nanomaterials. There is also a growing concern for public safety as well as ecosystem health.

1.2 Problem Identification

Cu Nanoparticles (Cu-NPs), Cu micron-size particles (Cu-MSPs) and Cu Oxide Nanoparticles (CuO-NPs) are already in use as additives in inks, lubricants, and metallic coatings. They are often emitted as particulates in smelters, metal foundries, and as torn particles from asphalt and rubber tires (Midander *et al*., 2009). With additional applications in the future, there is still no clear understanding regarding their long-term biological consequences. Only a few studies have attempted to thoroughly characterize Cu-NPs, Cu-MSPs and CuO-NPs and investigate the toxicological effects of direct exposure of cultured cells to these nano and micron-sized particles. Additionally, different physicochemical properties of the particles are likely linked to their toxicity. Therefore, it is necessary to thoroughly characterize the particles prior to toxicity assessment. Lastly, toxicity data are not typically extrapolated to account for different sized particles. This needs to be accomplished, as particles agglomerate upon suspension in aqueous environments.

1.3 Research Objectives

The purpose of this investigation was to thoroughly characterize Cu-NPs, Cu-MSPs and CuO-NPs upon their suspension in water and to determine the toxic effect of these copper nanoparticles on Murine Neuroblastoma (N2A) Cells. Specifically, the following issues were addressed:

1. Characterization of copper nanomaterial's physiochemical properties (morphology, shapes, agglomeration, spectral signature).

2. Toxicity assessment of Cu-NPs, Cu-MSPs and CuO-NPs on the murine neuroblastoma (N2A) cell line.

1.4 Research Focus

The focus of this basic research was limited to characterization of copper nanoparticles and micron-sized particles and the *in vitro* exposure of murine neuroblastoma cells to these copper nanoparticles. The goal was to gain a better understanding regarding the physicochemical properties of the copper nanoparticles prior to *in vitro* toxicity testing for future modeling and *in vivo* exposure studies and ultimately to develop recommended work place exposure limits.

1.5 Methodology

Prior to *in vitro* cell culture experiments, the effect of the cell culture media upon the copper nanoparticles was investigated. Previous research has demonstrated that suspension of nanoparticles in cell culture media generally leads to the aggregation of most compositions of nanoparticles (Murdock *et al*., 2008).

In vitro cell culture and aseptic techniques were used in this research. Murine neuroblastoma (N2A) cells were cultured in T-75 plastic flasks and exposed to various concentrations of Cu-NPs (25 nm), CuO-NPs (40 nm) and Cu-MSPs (500 nm) over certain time periods. The viability of the N2A cells after exposure to each type of Cu-NPs, Cu-MSPs and CuO-NPs at various concentrations was determined by measuring the mitochondrial function of the cell. Mitochondrial function acts as an indicator of metabolic activity and therefore also elucidates cell viability. The 3-(4,5-

dimethylthiazol-2-yl)-5-(3-carboxymethoxyphenyl)-2-(4-sulfophenyl)-2H-tetrazolium (MTS) assay was used for the assessment of cellular viability based on mitochondrial function.

Morphological characteristics of the cells after exposure to each type of Cu particle, were observed with three different imaging techniques – two forms of Scanning Electron Microscopy (SEM); high resolution and environmental, and two forms of Transmission Electron Microscopy (TEM); high resolution and low voltage. Agglomeration characteristics were observed by using Dynamic Light Scattering (DLS) in dosing media along with the endocytosis inhibitor Dynasore.

1.6 Assumptions/Limitations

(1) The properties of Cu and CuO NPs and Cu micron particles were expected to change after dry powder particles were suspended in water, dosing and growth medias.

(2) Cells dosed at the same Cu particle concentration were equally exposed throughout the experiment and that the exposure method used was satisfactorily conducted.

(3) Studying the toxicity of copper particles using neuroblastoma cells as a model has relevance to toxicity of the particles to humans.

(4) *In Vitro* results are limited and cannot be directly extrapolated without caution to predict *in vivo* results.

1.7 Implications

Nanoparticles are used more and more widely in both consumer products and the workplace. While researchers continue to study nanoparticles, a knowledge gap still exists. We need to ramp up efforts to determine health exposure risks as well as potential environmental effects. This research was conducted in order to elucidate copper nano- and micron-sized particles' properties to aid in the evaluation of acceptable exposure limitations in the occupational setting. Further investigations and measurements may help define control requirements and regulations for these and other nanoparticles. With the improved understanding and characterization of these particles we will be able to better define negative health and environmental effects prior to wide-scale use, thereby creating a healthier workplace environment for workers and consumers of nano- and nanobiotechnology.

1.8 Overview of Document

This document contains five chapters.

Chapter Two: A review of selected literature on current and future uses of nanoparticles including consideration for health and safety as well as an overview of copper toxicity. The literature demonstrates that the toxicity of Cu-NPs, Cu-MSPs and CuO-NPs can be characterized according to morphology, possibly size, cell viability assays, and studies comparing the toxicity of Cu particles to that of other particles.

Chapter Three: Provides a concise explanation of the methods used to obtain data.

Chapter Four: Presents an analysis and possible interpretation of the data obtained.

Chapter Five: Draws final conclusions and suggests future research.

II. Literature Review

2.1 Background

This literature review presents an overview on the basic background of nanoparticles, the current societal uses of nanoparticles and relevant health and safety considerations for the particles. A general summary of copper toxicity is provided as well as relevant disease associations and environmental fate of these particles. The literature review indicates that general conclusions can be drawn from cellular toxicity experiments with copper and shows that toxicity can be somewhat characterized according to cell viability, morphology, and size.

2.2 Nanoparticles (NPs)

Defined as particles with a diameter of less than 100 nm, nanoparticles are "a heterogeneous group of materials that differ in many characteristics and physiochemical properties, such as particle size, surface area, shape, morphology, elemental composition, solubility, and agglomeration state" (Midander *et al.*, 2009). Thus, in order to assess the *in vitro* and *in vivo* toxicity of nanoparticles, a number of different characterization methods are required.

The following illustration (Fig 2-1) provides examples of nanoarchitectures as well as research that has led to the manipulation of nanomaterials. The comparison between naturally occurring bio-structures and bio-molecules to manufactured nanostructures demonstrates the progress made in developing manmade structures that are comparable in size to the smallest natural materials.

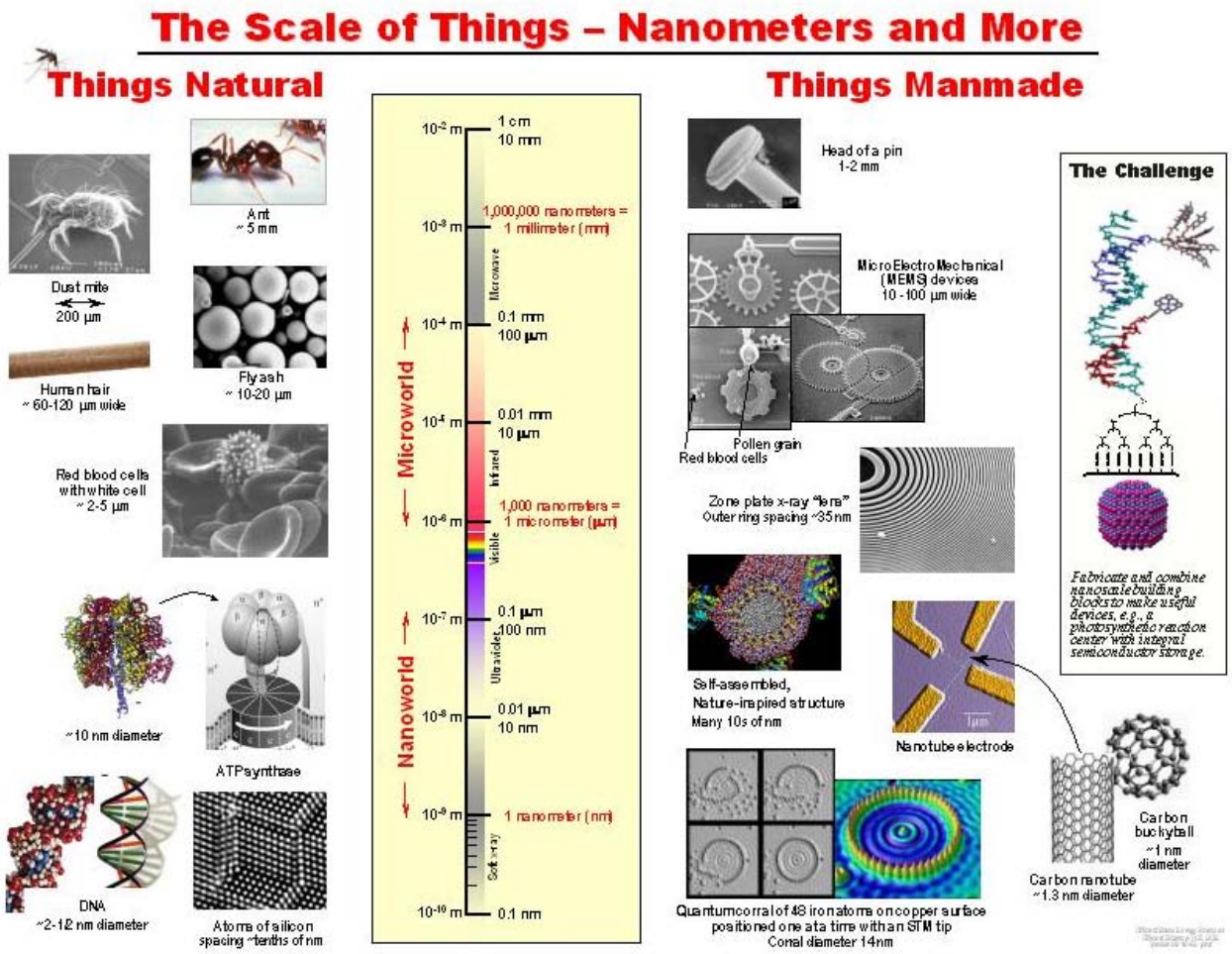

Fig 1. Comparison of things found in nature to nanostructures/nanomaterials
The above "Scale of Things" chart was designed by the Office of Basic Energy Sciences (BES) for the U.S. Department of Energy
(http://www.science.doe.gov/bes/scale_of_things.html)

The unique properties of nanoparticles are in large part a function of particle size. Smaller particles have a much larger surface area-to-volume ratio as well as number of particles in the same volume as compared to larger particles. Interestingly, this size difference equates to enhanced inflammatory response and increased toxicity for many nanoparticles when compared to larger particles of the same chemical composition (Oberdörster *et al*., 2005a).

From a toxicity perspective, the solubility of particles plays a two-fold role. While more soluble particles, such as dissolved metal in ionic form, may contribute to increased toxicity, more stable but less soluble forms of the metal may persist longer in bio-systems and thus bio-accumulate in both the organism and the environment ((Midander *et al*., 2009).

It is important to keep in mind that NPs are a heterogeneous group of materials that can vary widely due to size, morphology, shape, surface area, elemental composition, and solubility as well as agglomeration rate and sizes (Schrand and Hussain, 2010). There are many different types of nanoparticles that can be categorized based upon their composition into the following groups: 1) organic nanoparticles (e.g. polymers and dendrimers), 2) inorganic nanoparticles (e.g. metallic nanoparticles), 3) organic/inorganic hybrids (e.g. nanocomposites), 4) carbon based (e.g. functionalized fullerenes), 5) liposomes (e.g. functionalized, inclusion complexes), and 6) biological nanoparticles (e.g. protein and peptide- based nanoparticles with other biological components). Although almost all of these types of NPs have potential beneficial applications for the military, industry, and health sectors, there is still much unknown about potential hazards, safe handling practices, and effects on humans and the environment. Adverse health concerns include "cardiovascular and pulmonary diseases and an increased risk of developing lung cancer" (Midander *et al*., 2009).

2.2.1 Current and Future Uses

It is not possible to cover all the various applications of nanotechnology. In order to gain an understanding and appreciation for this area of research, a few specific

examples are highlighted here, including projected future uses. Table 1 shows an overview of some of the applications in nanotechnology (Schrand *et al*., 2010).

Table 1. Overview of Nanoparticle Types and Biotechnology Applications

Nanoparticle	Abbreviation	Application
Aluminum	Al	Fuel additive/propellant, explosive, wear resistant coating additive
Gold	Au	Cellular Imaging, Photodynamic Therapy
Iron (oxide)	Fe, Fe_3O_4, Fe_2O_3	Magnetic imaging, environmental remediation
Silica	SiO_2	Fabrication of electric and thermal insulators, catalyst supports, drug carriers, gene delivery, adsorbents, molecular sieves, and filler materials
Silver	Ag	Anti-microbial, Photography, Batteries, Electrical
Copper	Cu	Antimicrobial (ie. antiviral, antibacterial, antifouling, antifungal), antibiotic treatment alternatives, nanocomposite coating, catalyst, lubricants, inks, filler materials for enhanced conductivity and wear resistance
Cerium (oxide)	CeO_2	Polishing and computer chip manufacturing , fuel additive to decrease emissions
Manganese (oxide)	Mn	Catalysis, Batteries
Nickel (oxide)	Ni	Conduction, magnetic properties, catalysis, battery manufacture, printing inks
Titanium Dioxide	TiO_2	Photocatalyst, Antibacterial coating, sterilization, Paint, Cosmetics, Sunscreens
Zinc (oxide)	Zn, ZnO	Skin Protectant, Sunscreen

Nanotechnology may be the answer to our growing energy needs via the use of high-efficiency organic photovoltaics (OPVs). Nanostructered thin films, "composed of layers of semi-conducting organic materials (polymer or oligomers)" absorb photons from the solar spectrum and make up the OPVs (Dingman, 2005). Because OPVs composed of nanomaterials can be manufactured by a solution-based method they can be made much more cheaply than "inorganic" counterparts. Still, challenges exist before these devices can be mass produced, with the main concern being low solar energy

conversion efficiencies. Another area of energy research is in the area of fuel cells, because they are potentially more energy efficient than conventionally generated power. Researchers have started to use nanomaterials in the catalyst layer of fuel cells as they provide much larger active surface area due to their high surface areas. This increase in active surface area equates to an increase in the catalytic rate of oxidation or reduction while minimizing the amount of precious metals needed. In addition, researchers found that "the electrocatalytic properties of the materials are sensitive to particle size, so increased catalytic activity can be observed for nanoparticles and nanomaterials" (Minteer, 2005). However, one of the biggest benefits of using nanoparticles and nanomaterials is that the weight of precious metals is greatly reduced, and thus cost is also reduced. The need for a large amount of precious metals, thereby driving up cost, has been the major limitation of fuel cells (Minteer, 2005).

Nanopowders and nanoparticle dispersions make very uniform coatings because of their small and often homogenous size. Indium tin oxide and antimony tin oxide are well known coatings that provide optical transparency and electrical conductivity to materials. Examples of commercial uses include interactive touch screens and antistatic coatings utilizing the conductivity of the nanoparticles to dissipate the static charge. Nanoscale aluminum oxide and titanium oxide are also optically transparent and can greatly decrease abrasion when compared to traditional coatings. Other coatings of interest include zinc oxide and other rare-earth oxides that are also UV-reflective, but optically transparent, thus providing protection of surfaces from degradation due to UV exposures (Grocholl, 2005a).

Researchers have also been able to develop biosensors with near-infrared optical capability. For example, single-walled carbon nanotubes (SWNT) are able to "modulate their fluorescence emission in response to specific biomolecules" (Strano *et al*., 2005). A SWNT coupled enzyme bio-conjugate was used to detect glucose concentration by capitalizing on the fact that carbon nanotubes fluoresce in the near-infrared region and that human tissues and biological fluids are transparent to their emission. The sensor can then be employed to be excited by a near-infrared source from within the tissue and provide continuous blood glucose levels by producing the appropriate fluorescence response. The great potential benefit of this research is that the principle can be applied to many other chemical systems in order to develop new types of sensors for use in both medicine and biology (Strano *et al*., 2005).

SWNT have also been investigated for use in polymer composites. The main issue with composites containing nanotubes is the poor solubility of SWNTs in polymers, which can result in segregation. Therefore, successful SWNT composites require strong adhesion between the polymer matrix and SWNT as well as uniform dispersion within the matrix. In order to improve dispersion, coatings from surfactants and polymers are used to achieve "a) tighter bonding with the grapheme surfaces, b) miscibility with polymer matrixes of composites and c) substantially smaller concentration necessary for the preparation of SWNT dispersions" (Kotov, 2005).

Novel nanotechnology methods use layer-by-layer (LBL) nanoassembly composed of alternating oppositely charged polyelectrolytes, nanoparticles and proteins to create ultrathin multi-layer nano-capsules for targeted drug delivery. Examples of nanoparticles used successfully include different diameter and surface-charged gold,

silica, nanoclay-montmorillonite, alumina and titanium dioxide. Nanoarchitects need a wide variety of nanoparticles with varying properties and dimensions to proceed with this type of research. Ideally, good candidate nanoparticles are "monodispersed, stable in solution, charged nanoparticles of noble metals, metal oxides and ceramics with diameters of 5, 10, 20, 50 and 100 nm" (Lvov, 2005).

Continuous carbon or boron fiber-reinforced aluminum and magnesium, as well as silicon carbide reinforced aluminum belong in the category of metal matrix composites (MMCs). These MMCs have already been used in aerospace applications mainly due to their light weight and their ability to be tailored to possess specific properties. Metal matrix nanocomposities have improved physical and mechanical properties when compared to their micron-size counterparts. In addition, carbon nanotubes have "much higher strength, stiffness, and electrical conductivity as compared to metals, and therefore can significantly increase these properties of MMCs" (Rohatgi *et al.,* 2005).

Another area of interest is reducing the cost of producing these materials. Most of the research in synthesizing nanocomposites has involved the use of powder metallurgy techniques. This method is not only expensive, but also easily contaminated. Other methods of interest include stir mixing, squeeze casting and pressure infiltration that can be both rapid and inexpensive in producing large quantities of components that are of target sizes. Although there are still challenges in mixing nanoscale particles in metallic melts mainly due to agglomeration, several research teams have shown that there are dispersion techniques available (Rohatgi *et al.,* 2005).

It is easy to recognize the importance of nanotechnology and nanomaterial research just by the sheer amount of money being allocated to these fields. Lux Research

and the President's Council of Advisors on Science and Technology (PCAST) have shown that "the United States (US) is a global leader among governments funding nanotechnology" (A Matter of Size: Triennial Review of the National Initiative, 2006). It is important to keep in mind that it is complicated to compare nations' spending on nanotechnology due to differences in calculating and budgeting expenditures. Various nations have different benchmarks in reporting what is public and private funding, how researchers' salaries are defined, etc. As seen in Fig 2-2, the United States leads in nanotechnology research spending, although that position is being challenged. However, according to Cientifica's 2003 *Nanotechnology Opportunity Report*, Japan's launch of the Nano-Business Creation Initiative for creating new nanotechnology businesses in Japan and building their foundation as nanotechnology leaders of the future indicate that they also aspire to be a global leader in nanotechnology (A Matter of Size: Triennial Review of the National Initiative, 2006).

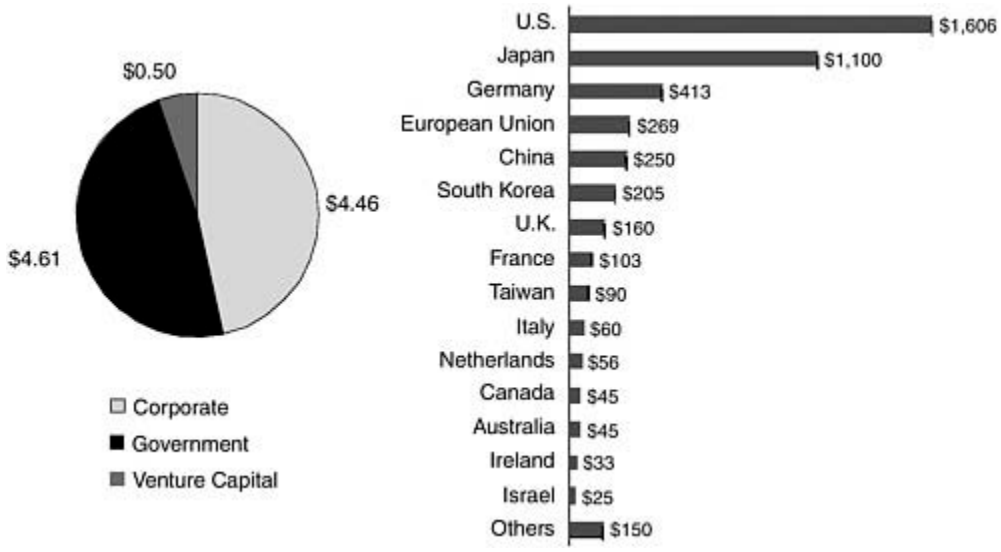

Fig 2. World nanotechnology funding, 2005. (Left) Nanotechnology funding globally by source, 2005 (U.S. $ billion). (Right) Government nanotechnology funding by country, 2005 (U.S. $ million). SOURCE: Lux Research, Inc. 2006. The Nanotech Report. 4th Edition. New York: Lux Research, Inc.

A more recent look at nanotechnology spending shows that more than 60 countries now have their own nanotechnology programs. These nations are most likely following the lead of the United States, who announced establishment of the US National Nanotechnology Initiative (NNI) in 2000. In 2010, nine years after the initiation of the NNI, US federal spending dollars on nanotechnology has jumped from $464 million in 2001 to $1.8 billion (Shapira & Wang, 2010).

More spending in turn leads to more research publications. In fact, Shapira & Wang (2010) identified more than 91,500 nanotechnology articles published between August 2008 and July 2009 worldwide. However, even though the publications featured researchers from 152 countries, 90% of the papers were written by authors from only 15 countries. The top four countries by author contribution are the United States (23%), China (22%), Germany (8%), and Japan (8%) (Shapira & Wang, 2010).

As seen in Fig 2-3, while the US remains the focal point on the nanotechnology map, US researchers partner with Chinese colleagues most often; although a strong cluster of collaboration efforts are also seen with some European countries. However, even after ten years since the launch of the NNI, only a small number of countries still sponsor much of the world's nanotechnology research; nanotechnology research has yet to become a global activity. With competing technologies and limited funding, future

nanotechnology research will most likely not keep pace with the explosive growth of the past decade. Shapira and Wang (2010) recommend more high-quality international collaborations for interested stakeholders to increase alliances with colleagues in other countries.

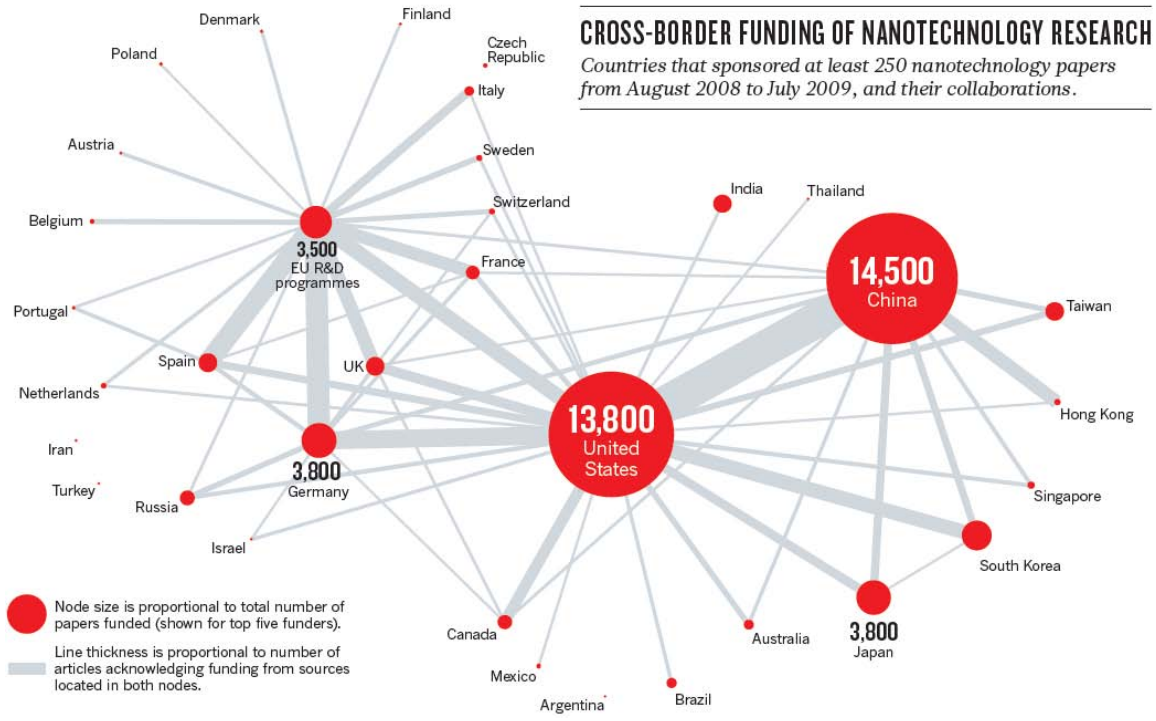

Fig 3. A graphical depiction of nanotechnology research papers funded, with the node size being proportional to the total number of papers (Shapira & Wang, 2010).

2.2.2 Uses of Copper Nanoparticles

In our recent medical history, fungal infections have become a major health concern especially in immune-compromised patients such as those with acquired immune deficiency and patients undergoing chemotherapy treatment. Concurrently, copper nanoparticles have been investigated for use in biotechnological applications that may

one day combat some of these disease conditions. For example, researchers have combined copper nanoparticles with a polymer material to make a composite capable of releasing metal species in a controlled manner in order to inhibit the growth of fungi and other pathogenic microorganisms (Cioffi *et al*., 2005).

The germicidal properties of copper have been well recognized, in both its particulate and soluble forms. Copper and copper oxide dispersions have been used in maritime industries since the 19th century in antifouling coatings. The downside to this application is the eventual mass release of copper compounds into the maritime system. However, more recently, Cioffi *et al.* (2005) proposed a similar strategy as a way to control the growth of *saccharomyces cerevisiae* yeast and molds through the use of nanocomposites with spinning coatings that are equipped to release copper. They conclude that this nanostructured coating seem to be very promising as there is the capability to control the metal release (Cioffi *et al*., 2005). Another area of interest is the incorporation of low-copper-loading materials into packaging materials for food. Furthermore, copper oxide nanopowder has also been suggested as an anti-microbial preservative for use in wood and food products (Grocholl, 2005b).

In addition to controlling the growth of yeasts and molds, Cu-NPs have also been shown to be effective in controlling the growth of bacteria such as *Escherichia coli* and *Bacillius subtilis*. The theorized mechanism of Cu-NPs acting as an antibacterial agent is "due to the interactions with the SH groups leading to protein denaturation" (Schrand *et al.*, 2010).

Manufactured nanosized copper particles have also been used as additives in lubricants, inks, polymers and plastics, as well as metallic coatings. They provide

excellent lubrication in oil due to mending effects and as an additive they reduce friction as well as wear and tear on surfaces (Liu *et al.*, 2004). In lithium ion batteries, nanosized copper particles are deposited evenly onto graphite surfaces as an anode material (Guo *et al.*, 2002). Copper has also been used in various skin products to enhance healing and prevent infection (Midander *et al*., 2009).

2.3 Health and Safety Considerations for NPs

As mentioned earlier, the National Nanotechnology Initiative (NNI) is a federal interagency committee that was established in 2000 with aims to "expedite the discovery, development, and deployment of nanotechnology in order to achieve responsible and sustainable economic benefits, enhance the quality of life, and promote national security" (A Matter of Size: Triennial Review of the National Initiative, 2006). The NNI has outlined goals to ensure responsible development of nanotechnologies and the conduct of responsible research. Some of NNI goals include carrying out research in order to "characterize environmental, health, and safety (EHS) impacts of the development of nanotechnology and assessment of associated risks", educational efforts directed at undergraduate programs and public outreach, and research aimed to identify and quantify nanotechnology implications in a broader societal, economical, ethical, legal and occupational contexts (A Matter of Size: Triennial Review of the National Initiative, 2006).

However, thus far, the committee has found that the Environmental, Health, and Safety (EHS) effects data thus far produced by nanotechnology research are inconclusive. The NNI state that risk assessments are poorly defined and need to be further developed.

In addition, more research must be conducted to assess for EHS hazard potentials from various nanomaterials. Ambiguous results were also obtained on the health and well-being of laboratory animals. Lack of *in vitro* and *in vivo* studies are partially to blame for the deficiency in thorough characterization of nanomaterials. Achieving the goal of obtaining valid and reproducible EHS data will depend on further research to produce more specific risk-based guidelines. Until this goal can be met, the committee suggests precautionary measures in order to protect all nanomaterial workers, the public, and the environment. Addressing the social and ethical challenges of nanotechnology will involve the collaboration of scientists, engineers, toxicologists, and policymakers. Throughout this national effort, it is important for the public to remain engaged in order for risks to be adequately addressed and communicated and to ensure that nanotechnology research is carried out in a responsible manner (A Matter of Size: Triennial Review of the National Initiative, 2006).

As applications in nanotechnology continue to expand and consumers find more and more nanoparticles in everyday products the area of health concerns will also gain considerable attention. Thus far, most of the studies related to nanoparticles have been focused on respiratory exposures. Other exposure routes including dermal and ingestion have also started to be considered as potential routes of concern. A likely scenario for ingestion to occur as a secondary route of exposure may involve mucociliary escalator action where nanoparticles originally cleared by the respiratory tract are then ingested. In addition, “nanomaterials can be ingested directly via water, food, cosmetics, drugs, drug delivery devices, etc (Chen *et al.*, 2006). Studies have also indicated that differing sized nanoparticles may induce various toxicological effects after gastrointestinal intake.

2.3.1 Physicochemical Characteristics vs. Biological Activity

High surface area to volume ratio is a highly desirable aspect of nanoparticles, such as in catalytic reactions, but one which can also have grave effects in terms of toxicity. An analogy can be drawn from the ratio of surface area to volume of molecules or atoms to that of the potential biological and chemical activity from nanoparticles. With decreasing particle size, this ratio increases by orders of magnitude as seen in Table 2.

Table 2. Particle number and particle surface area per 10 µg/m³ airborne particles (Oberdörster *et al*., 2005b).

Particle diameter (µm)	Particle no. (cm^{-3})	Particle surface area ($\mu m^2/cm^3$)
5	153,000,000	12,000
20	2,400,000	3,016
250	1,200	240
5,000	0.15	12

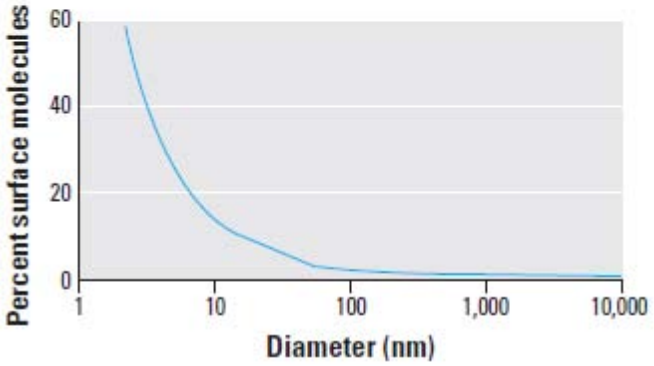

As seen in Table 2, surface molecules are plotted as a function of particles' diameters. At less than 100 nm, surface molecules increase exponentially with a decrease in particle diameter. This results in a massive increase in chemical and biological activity potential. It is important to understand that this is a two-sided issue. On the one hand, increased biological activity can be very beneficial for "antioxidant activity, carrier capacity for therapeutics, and penetration of cellular barriers" (Oberdörster *et al*., 2005b). However, toxicity and oxidative stress of cellular functions may also dramatically increase.

2.3.2 Benefits vs. Occupational Exposure Risks

While the benefits of nanoparticles are indeed promising, the many useful properties of nanoparticles (size, surface area, reactivity) also pose a number of risks. Currently, a rising number of workers are potentially exposed to nanomaterials in "research laboratories, start-up companies, production facilities, and in operations where nanomaterials are processed, used, disposed or recycled" (Howard, 2005). Many challenges remain in the determination of potential negative health effects and occupational safety risks from working with intentionally produced and engineered materials and devices. But the larger goal is to realize potential benefits of nanotechnology research while being meticulously careful in minimizing risks associated with these endeavors (Howard, 2005).

2.3.2 Regulations

In terms of regulation requirements set forth for nanomaterials the issue is somewhat unclear. The EPA has mainly focused its efforts towards regulating nanomaterials through the Toxic Substances Control Act (TSCA) where most materials are considered as chemical substances. The regulatory approach used by the EPA follows a four-pronged approach that includes the following: pre-manufacture notifications, a significant new use rule, an information gathering rule, and a test rule (TSCA, U.S. EPA, 2011).

Prior to the manufacturing of new chemical substances, companies must provide specific information to the EPA as required by TSCA. The EPA then takes action to ensure that human and environmental contamination risks are minimized. The EPA provides assistance to manufacturers when determining whether their nanomaterials fall under the new chemical category. Since 2005 the EPA has reviewed over 100 new notifications for nanomaterials, and this number is expected to continue to rise. The agency has taken a number of actions including "limiting the uses of the nanoscale materials, requiring the use of personal protective equipment, such as impervious gloves and NIOSH approved respirators, limiting environmental releases, and requiring testing to generate health and environmental effects data" (TSCA, U.S. EPA, 2011).

It is important to note that there are exceptions made for certain manufacturers of new nanomaterials under certain conditions where possible exposures are very tightly controlled and risks are minimized to include environmental releases. Another proposed rule developed under TSCA section 8a requires submission of additional information from manufacturers such as production volume, methods used, exposures and any relevant release information and all available safety data. Lastly, under TSCA section 4

the EPA proposed a testing rule for certain nanomaterials already in use. Any new information on nanomaterials not already being tested by other Federal agencies would enable the agency to further understand any novel toxicity data that link certain chemical and physical characteristics to *in vitro* and *in vivo* toxicity (TSCA, U.S. EPA, 2011).

2.3.2 Future Concerns and Funding

The NIOSH Nanotechnology Research Center (NTRC) was established in 2004 largely due to the anticipated increase in current as well as future nanotechnology research developments and to study potential worker exposures. NIOSH scientists form the bulk of NTRC researchers engaged in developing future NIOSH guidelines in nanotechnology health research. A far-reaching collaboration effort from the combined efforts of government agencies, academia and the private sector has aided the development of a NIOSH strategic plan in nanotechnology research and guidance (Howard, 2005).

The strategic plan's goals are as follows:

1. Determine if nanoparticles and nanomaterials pose risks for work-related injuries and illnesses.

2. Conduct research to prevent work-related injuries and illnesses due to nanotechnology products.

3. Promote healthy workplaces through interventions, recommendations, and capacity building.

4. Enhance global workplace safety and health through national and international collaborations on nanotechnology research and guidance.

The NIOSH Office of Extramural Programs (OEP) works with the research community and awards grants in occupational safety and health grants. To date, OEP has committed roughly 5.3 million dollars to nanotechnology research. NIOSH also joined with the Environmental Protection Agency as well as the National Science Foundation in 2004 and committed $7 million in funding of grants in continued research (Howard, 2005).

2.3 Copper Toxicity

As a naturally occurring metallic compound, copper may exist by itself or may be associated with other elements. Copper particulates released into the air may be from both natural and anthropogenic sources. Volcanic eruptions are the main natural source of windblown copper particulates in dust. Copper smelters or other ore processing facilities are sources of copper particulates from manufacturing processes. Many times copper particles are removed from the atmosphere by precipitation, but they can be easily re-suspended in the form of copper dust. In the U.S., the mean ranges of copper in the ambient air can vary widely, from 5 to 200 ng/m^3 (ATSDR, 2004).

Copper releases into the waterways usually occur via natural weathering of soil and rocks or from anthropogenic sources such as the effluent of industries or sewage treatment plants. Copper concentrations in drinking water may vary depending on pH and hardness of the local water. Copper values in soil vary from 5 to 70 mg/kg and the estimated daily value of ingestion intake of copper from food is 1.0-1.3 mg/kg for adults (0.014-0.019 mg/kg/day). The Food and Nutrition Board of the Institute of Medicine recommend dietary allowance (RDA) of “340 micrograms (μg) of copper per day for

children aged 1–3 years, 440 μg/day for children aged 4–8 years, 700 μg/day for children aged 9–13 years, 890 μg/day for children aged 14–18 years, and 900 μg/day for adults" (ATSDR, 2004).

Copper is a necessary trace element in the body, and mechanisms have evolved for the use, transport, and excretion of copper from the body. Copper is an essential nutrient because it is incorporated as one of many metalloenzymes necessary for proper hemoglobin formation, carbohydrate metabolism, collagen, elastin and hair keratin, antioxidant defense, etc,. Normal copper absorption occurs from the stomach and small intestine. Complexing molecules have been known to exist in blood, but researchers have only been able to discover cellular copper transporters in the last decade or so. For those individuals lacking the proper copper exporter pump, diseases such as Menkes or Wilson's diseases result (Nordberg et al, 2007).

2.4.1 Environmental Contamination

As manufactured nanomaterial use increases in many commercial products, concerns have been raised regarding environmental release and contamination. Because of their highly reactive nature, nanoparticles differ in many physical and chemical characteristics from their metallic ion counterparts. Ganesh *et al.* (2010) evaluate nanocopper removal and the related toxicity in municipal wastewaters. They note that wastewater treatment plants are most likely the last barrier to any nanomaterial release into the environment. It is important to note that because of aforementioned differences of nanoparticles from metal ions, they also behave differently in biosolids. In fact,

wastewater effluents models have already detected nanomaterial presence (Ganesh *et al*., 2010).

Ganesh *et al.* (2010) conducted two sets of experiments evaluating copper nanoparticle and copper ion removal, one with normal activated sludge microorganisms and one with activated sludge filtrates that did not contain biomass. The objective was to observe the amount of copper removal without the aid of biosorption. For the first experimental condition, approximately 30-70% of copper ions were removed. Cu NPs were removed at a higher percentage of around 90%. Interestingly the team observed that nearly 25-55% of copper ions and 75-80% of CuNPs were removed in the activated sludge filtrates without biomass. This indicates that copper biosorption was not a significant mechanism of copper removal.

This preliminary study gives only rudimentary understanding of the fate and transport of CuNPs during wastewater treatment; other impacts including long-term effects are unknown. Further concerns include changes to the microbial community of the activated sludge that may result from prolonged exposure to CuNPs. Other mechanisms may take place, further altering CuNPs and other nanomaterials at the point of environmental release and during sludge handling and ultimately disposal. Lastly, it was found that all residual samples of copper violated the National Toxics Rule (NTR) criteria for wastewater discharge of 8.9 µg/L (Ganesh *et al*., 2010).

2.4.2 Exposure and Human Disease

Many studies have found a number of systemic effects including gastrointestinal,

hepatic, as well as renal effects following acute, intermediate, and chronic exposures to copper and an extensive database exists on the toxicity of ingested copper in animals, including immunological and developmental effects. However, several studies have attempted to investigate potential neurological and reproductive targets, without conclusively finding any effects (ATSDR, 2004).

The general population comes in contact with copper through ingestion of food and water, and dermal contact with air, water or soil that contains copper. Although contact primarily occurs from intake, the amount of copper uptake is usually less than the average dietary requirements (RDAs) for copper. Inhalation of copper is a concern for individuals living near copper smelters or other refineries. Workers in these facilities may experience high occupational exposures to copper. Another concern is young children ingesting soil with high levels of copper while living near these facilities. The EPA has identified copper hazards at 906 of 1,647 hazardous sites on the EPA's National Priorities List (EPA NPL) (ATSDR, 2004).

Ingestion of excess copper is a concern because copper is easily absorbed from the stomach and the small intestine. There are, however, several mechanisms for dealing with copper overload. Excess copper that is absorbed in the intestinal mucosal cells binds to the metal binding protein metallothionein. When the mucosal cells slough off the copper is also excreted. The remaining copper in the system is then transported to the liver, and then becomes a part of the bile that will ultimately be excreted in feces. Copper homeostasis can be fairly effective in the body. However, excess copper can result in serious damage to the body including "liver and kidney damage, anemia, immunotoxicity, and developmental toxicity" (ATSDR, 2004). Excess copper that

cannot be mediated by homeostatic processes of the body will even bind with several enzymes to interfere with the protective mechanisms of cells from free radical damage (ATSDR, 2004).

For drinking water, the EPA has determined that it should not contain more than 1.3 mg of copper per liter of water (1.3 mg/L). The Occupational Safety and Health Administration (OSHA) has set a limit of "0.1 milligrams/cubic meter (mg/m^3) for copper fumes (vapor generated from heating copper) and 1.0 mg/m^3 for copper dusts (fine metallic copper particles) and mists (aerosols of soluble copper) in workroom air to protect workers during an 8-hour work shift (40-hour workweek)" (ATSDR, 2004).

2.4.2.2 Respiratory and Gastrointestinal Distress

While copper can be irritating to the respiratory tract, the most commonly reported adverse health effect is gastrointestinal distress. Workers routinely exposed to copper dust have reported increased coughing, sneezing, running nose, fibrosis and generally increased vascularity in the nasal cavity. Nausea and abdominal pain have been reported after drinking fluids high in copper, stagnant water from a first-draw copper pipe (such as first thing in the morning without any flushing of the water), or beverages stored in a copper container (ATSDR, 2004).

2.4.2.3 Nervous System Effects & Neurological Disorders

Murthy *et al.* (1981) conducted a study by administering either manganese chloride (1 mg manganese/mL drinking water) or copper sulfate (250 mg copper/kg food) to growing rats for 30 days. The rats are normally maintained on a 10% casein diet.

Neurobehavioral performances remained the same for the rats exposed only to copper in their diets but the combined exposure to copper and manganese produced elevated levels of dopamine and norepinephrine and a depression of 5-hydroxytryptamine, a dopamine metabolite. These changes suggest that copper may adversely affect the nervous system but the study was inconclusive and suggested that further research be conducted to investigate the neurotoxic potential of copper (Murthy *et al.,* 1981).

2.5 Neuroblastoma in Humans

The cells used in the cellular experiments were Murine Neuroblastoma (N2A) cells. Neuroblastoma in humans, occurs mostly in infants and children and is a cancerous tumor that develops from nerve tissues. Since nerves run throughout the body, this disease can also occur in many areas of the body. Neuroblastoma tumors usually develop in tissues forming the sympathetic nervous system (PubMed Health, 2011).

For children less than 15 years of age, sympathetic nervous system tumors account for 7.8% of all tumors, with most of the cases being neuroblastomas. Neuroblastomas are also the most common cancer of infancy, with double the incidence rate of the next most common disease in the first year of life: leukemia (National Cancer Institute, 2011). Most of the tumors originate in the adrenal gland in the abdomen, close to the spinal cord, or sometimes in the chest area. Unfortunately, the disease can easily metastasize to other regions, including bones of the extremities, head, pelvis, and shoulders as well as bone marrow, liver, skin, and lymph nodes (PubMed Health, 2011).

Survival for children diagnosed at age 1 to 4 is 83% and 40% for those 5 years or older. The cause of neuroblastoma is largely unknown. Certain medications, maternal

use of alcohol and tobacco and paternal occupational hazards have associations, but these are not clear (National Cancer Institute, 2011). The diseases occur slightly more in boys than girls.

III. Methodology

3.1 Introduction

The goal of this research was to characterize three copper nano and micron-sized particles and observe the particles' relevant toxicity effects on N2A cells. The characterization was carried out using a series of methods and equipment. Malvern's Zetasizer was used for Dynamic Light Scattering (DLS) to characterize the average size of agglomerates in the dosing media. A dark-field microscope with Cytoviva as a light source and using the Hyperspectral Imaging (HSI) technique was used for verifying that the particles are indeed copper particles by analyzing the spectra collected by the spectrophotometer. The Low Voltage Electron Microscope (LVEM), Environmental Scanning Electron Microscope (ESEM), Scanning Electron Microscope (SEM) and Transmission Electron Microscope (TEM) were used to observe surface morphology changes that the particles experience over time while suspended in water, oxidation changes on particle surfaces, uptake of particles into N2A cells, and also confirmation of sizes as well as any possible changes in particle size over time. The 3-(4,5-dimethylthiazol-2-yl)-5-(3-carboxymethoxyphenyl)-2-(4-sulfophenyl)-2H-tetrazolium (MTS) assay was used for the assessment of cellular viability based on mitochondrial function for the Cu-NP 25 nm, CuO-NP 40 nm, Cu-MSP 500 nm, as well as $CuCl_2$.

3.2 Assumptions

Several key assumptions were made at the beginning of the laboratory experiments.

(1) The properties of Cu and CuO NPs and Cu micron particles were expected to change after dry powder particles were suspended in water, dosing and growth medias.

(2) Cells dosed at the same Cu particle concentration were equally exposed throughout the experiment and that the exposure method used was satisfactorily conducted.

(3) Studying the toxicity of copper particles using neuroblastoma cells as a model has relevance to toxicity of the particles to humans.

(4) *In Vitro* results are limited and cannot be directly extrapolated without caution to predict *in vivo* results.

3.3 Cell Line

The Neuro-2a (N2A) line was obtained from the American Type Culture Collection (ATCC). Clone Neuro-2a was derived by R.J. Klebe and F.H. Ruddle from a spontaneous tumor of a strain A albino *Mus musculus*, or mouse. These cells are adherent type cells, and their morphology is described as neuronal and amoeboid stem cells. The disease that these cells would eventually manifest to would be neuroblastoma in the organism. ATCC product description indicates that this tumor line produces large quantities of microtubular protein which researchers believe "play a role in a contractile system which is responsible for axoplasmic flow in nerve cells" and that the World Organization for Animal Health (OIE) routinely uses these cells for the diagnosis of rabies (ATCC, 2011). These cells were chosen because they provide a neuronal model,

bringing a different perspective than the more commonly studied macrophages or keratinocytes.

3.4 Cell Culture

Cells were maintained in Dulbecco's Modified Eagle's Medium (DMEM) nutrient mixture F-12 Ham's and supplemented with 10% Fetal Bovine Serum (FBS), received from American Type Culture Collection (ATCC, Manassas, USA). 1% Penicillin-Streptomycin, received from American Type Culture Collection (ATCC, Manassas, USA) was added to the growth media. DMEM was freshly prepared from powder form and preparation instructions were followed from Sigma-Aldrich's product information page (Sigma-Aldrich, DMEM, 201). Fetal Bovine Serum is widely used as a growth supplement for cell culture use mainly due to its high content of embryonic growth promoting factors. From Sigma-Aldrich, "when used at appropriate concentrations it supplies many defined and undefined components that have been shown to satisfy specific metabolic requirements for the culture of cells" (Sigma-Aldrich, 2011). Penicillin-Streptomycin (pen strep) is a broad-spectrum bactericide effective against both gram negative as well as gram positive bacteria. Upon thawing its activity decreases. Therefore, it's best that it is thawed shortly before use (Lonza, 2011).

3.4.1 Cell Maintenance

Cell maintenance was conducted to ensure healthy cells were always available for experiments. Detailed cell care instructions are given in appendices A and B.

3.4.2 Cell Count/Cell Volume

In order to measure and compare results, and to ensure quality imaging, cells must be plated at certain concentrations. Unless otherwise noted, all cells are plated in 96-well plates at 150K cells per mL. Nexcelom Bioscience's Cellometer Vision was used for automated cell counts. Samples can also be adjusted to the desired concentration in the program (Nexcelom Bioscience, 2011).

3.5 Biotek Synergy HT

The water-soluble formazan product produced by active mitochondria in live cells was quantified with the Biotek Synergy HT plate reader in the MTS assays. The plate reader measured emitted light at 490 nm wavelengths for the MTS assay. A reading at "0" minutes was also taken and then subtracted from the final reading to account for any background absorbance due to the nano or micron-sized particles or the solution. The percent reduction of MTS was then compared to the control cells not exposed to treatment, which represented 100% of MTS reduction.

3.6 Nanoparticles

The test materials, Cu-NPs (small metallic Copper nanoparticles 25 nm, small oxidized Copper nanoparticles 40 nm in diameter) and Cu micron-sized particles (large Copper particles at 500 nm in diameter) were supplied by American Elements. The Cu nano and micron particles, in dry powder form, were suspended in de-ionized water to make stock solutions (1 mg/ml). Prior to each use, stock solutions were sonicated to

reduce agglomeration of particles. Agglomeration was characterized with the Olympus IX71 inverted fluorescent microscope with CytoViva as a light source (Appendix G).

Fresh dilutions were made for each specific experiment from stock solutions and the appropriate concentrations were obtained by mixing the appropriate amount of stock solution with dosing media. Details for each copper concentration (dose) are given in future sections. Tables 3 and 4 categorize nanoparticles by source, size, assay use, and dosing range. Other dosing concentrations are given specifically for the specific result reported in the results section.

Table 3. Nanoparticles Used

Chemical	Size (diameter)	Source	Uses
Cu	25 nm	American Elements	Characterization, MTS Assay
CuO	40 nm	Sigma Aldrich	Characterization, MTS Assay
Cu	400 nm	American Elements	Characterization, MTS Assay
$CuCl_2$		Novacentrix	MTS Assay

Table 4. Nanoparticle Dosing (0, 5, 10, 25, 50, 100 µg/mL media) (10% FBS) (1% Penicillin-Streptomycin) for MTS Assay

Particle	0 µg/mL	5 µg/mL	10 µg/mL	25 µg/mL	50 µg/mL	100 µg/mL
Cu 25 nm	3 mL of dosing media	15 µL Cu 25 nm + 2985 µL dosing media	30 µL Cu 25 nm + 2970 µL dosing media	75 µL Cu 25 nm + 2925 µL dosing media	150 µL Cu 25 nm + 2850 µL dosing media	300 µL Cu 25 nm + 2700 µL dosing media
CuO 40 nm	3 mL of dosing media	15 µL CuO 40 nm + 2985 µL dosing media	30 µL CuO 40 nm + 2970 µL dosing media	75 µL CuO 40 nm + 2925 µL dosing media	150 µL CuO 40 nm + 2850 µL dosing media	300 µL CuO 40 nm + 2700 µL dosing media
Cu 500 nm	3 mL of dosing media	15 µL Cu 500 nm + 2985 µL dosing media	30 µL Cu 500 nm + 2970 µL dosing media	75 µL Cu 500 nm + 2925 µL dosing media	150 µL Cu 500 nm + 2850 µL dosing media	300 µL Cu 500 nm + 2700 µL dosing media
$CuCl_2$	3 mL of dosing media	15 µL $CuCl_2$ + 2985 µL dosing media	30 µL $CuCl_2$ + 2970 µL dosing media	75 µL $CuCl_2$ + 2925 µL dosing media	150 µL $CuCl_2$ + 2850 µL dosing media	300 µL $CuCl_2$ + 2700 µL dosing media

3.7 MTS Assay

The 3-(4,5-dimethylthiazol-2-yl)-5-(3-carboxymethoxyphenyl)-2-(4-sulfophenyl)-2H-tetrazolium (MTS) assay is a colorimetric method for the assessment of cellular viability based on mitochondrial function. The assay consists of the novel tetrazolium compound and an electron coupling reagent phenazine methosulfate (PMS). Cells bioreduce the MTS into a formazan product that is tissue culture soluble. This chemical conversion process can be seen in figure 3-1 below. The absorbance of the formazan product was measured at 490 nm directly from the 96-well assay plates.

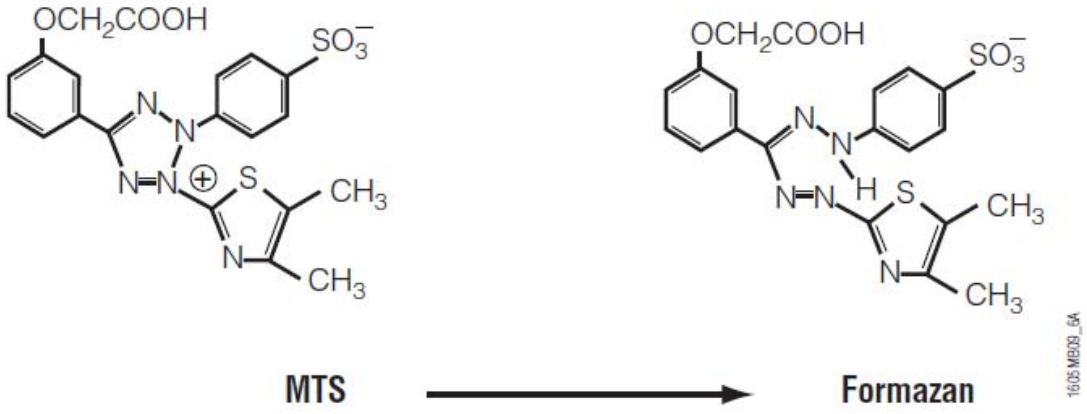

Figure 4. Structure of MTS tetrazolium salt and the formation of the Formazan product. ("Cell Titer 96® Aqueous Non-Radioactive Cell Proliferation Assay", Promega, 2009).

Four 96 well plates of N2A cells were treated with the three types of Cu particles as well as $CuCl_2$. The same amount of dosing media was placed in cell wells to be used as controls. After 180 minutes of treatment and incubation with the copper particles the MTS was added to all the cell wells. At "0" time a reading was taken at 490 nm as a

background. After an hour of incubation with the MTS agent, a dark purple color developed within the cells, indicating the formation of a water-soluble formazan product by active mitochondria in live cells. The formazan product was quantified with a microplate reader at 490nm. A “0” minute reading was then subtracted out of the final reading to account for background absorbance due to the NPs or the solution. The percent reduction of MTS was compared to controls (cells not exposed to particles), which represented 100% MTS reduction.

The MTS experiment was then repeated, but this time with a 1 hour pre-treatment with the endocytosis inhibitor Dynasore. More information on Dynasore can be found in section 3.8.5 along with the Dynamic Light Scattering technique. This experiment was conducted in order to eliminate con-founders and determine whether pre-treatment with Dynasore can increase cell viability prior to Cu exposures.

3.8 Characterization

Characterization of the copper particles was conducted in a series of phases using different techniques. The goal of characterization was to study particle morphology and surface oxidation in “dry” as well as “wet” conditions. A series of techniques were used, beginning with the Low-Voltage Electron Microscope (LVEM) and proceeding to the Environmental Scanning Electron Microscope (ESEM), the Scanning Electron Microscope (SEM), the high resolution Transmission Electron Microscope (TEM), Dynamic Light Scattering (DLS), and finally Hyperspectral Imaging (HSI), in turn.

3.8.1 LVEM

Low Voltage Electron Microscopy was conducted for the Cu-NP 25 nm, CuO-NP 40 nm, and Cu-MSP 500 nm. The LVEM is designed for a broad range of applications in many fields to include biology, medicine and material science and provides valuable capabilities in nanotechnology and organic materials. High contrast is achieved by using much lower electron energy at 5 keV compared to the high resolution TEM and as a result there is additional electron scattering resulting in better contrast (Schrand and Hussain, 2010).

The LVEM was used as a basic tool to observe the particles and provide an estimate of the sizes of the particles. It serves as a preliminary scan and gives a basic view of the general shapes of the particles. The LVEM is under high vacuum but uses low voltages. The table-top set up also provides for ease of use.

3.8.2 ESEM

The ESEM was used to better observe morphology. It is a unique instrument as the samples can be studied with it while they are somewhat “wet”. Limited surface morphology can be observed. The ESEM permits increased magnification of images but operates under low vacuum conditions.

3.8.3 SEM

An experiment evaluating N2A cells exposed to various copper particles as well as $CuCl_2$ was conducted. The N2A cells were seeded on glass cover slips and allowed to grow for about 24 hours or when they looked fairly confluent and healthy. Samples were

then exposed to the particles or $CuCl_2$ for 3 hours and then washed and dried. Samples were then prepared for imaging at the Materials Lab. Further details on this protocol can be found in appendix E.

3.8.4 TEM

Dry characterization was conducted using the high resolution TEM. Cu Nanoparticles (Cu-NPs) (25 nm), Cu micron-size particles (Cu-MSPs) (500 nm) and Cu Oxide Nanoparticles (CuO-NPs) (40 nm) were freshly suspended in water and prepared for TEM imaging at the "0" time point. Samples of each type of particle were then imaged again at a short term incubation time point (2 or 3 months) and again at a long term incubation time point (6 months). This incubation time point imaging was conducted in order to look for general morphology changes, as well as surface morphology changes and surface oxidation changes.

3.8.5 Dynamic Light Scattering

Prior to any experimentation with the N2A cells, it was important to learn about the behaviors of the particles in dosing media, replicating the conditions the cells would experience while being dosed. In order to understand biochemical interactions, it was necessary to investigate solution agglomeration of particles. Agglomeration of particles may interfere with cellular uptake by processes such as phagocytosis or pinocytosis. To eliminate possible confounding factors due to bio-molecule size, only dosing solution (without FBS) was added to formulate solutions for measurements.

To do this, Malvern's Zetasizer was used to conduct dynamic light scattering of the Cu particles. In order to understand whether the cells would uptake the particles, it is necessary to study particle behavior and agglomeration in just the dosing media alone as large agglomerates would not be able to cross the cell membrane. The Zetasizer DLS instrument measures particle size by looking at the diameter of the sphere that diffuses at the same speed as the particle being measured. The instrument first measures the Brownian motion of the particles and then interprets this data using the Stokes-Einstein equation to determine the relationship between the size of the particle and its speed due to the Brownian motion. The particles are in constant motion, and the speckle pattern that is created will also appear to move. Constructive and destructive phases of the scattered light will in turn cause bright and dark areas. These areas grow and diminish in intensity and will appear to fluctuate. The DLS system measures this rate of fluctuation and uses this information to calculate the size of the particles (Malvern Zetasizer Manual, 2009).

The Cu particles were freshly prepared from stock solutions to arrive at final concentrations of 25 ug/mL, 50 ug/mL and also 100 ug/mL and added to 25 μM of Dynasore, an endocytosis inhibitor. Dynasore, an endocyctosis inhibitor, is co-incubated with the particles because current research shows that it may potentially aid cell viability while the cell is dosed with Cu nanoparticles (Schrand *et al*., In Preparation). Specifically the addition of Dynasore increases viability of cells dosed with metallic forms of Cu at high doses (>50 μg/ml).

From studies conducted by Schrand et al. (In Preparation), it was discovered that both small and large metallic Cu- NPs are more toxic than the CuO-NPs. Additionally, CuO-NPs are not toxic after 3h of exposure and are also not affected by the presence or

absence of the endocytosis inhibitor. This observation poses the possibility that if the chemical modulator can affect the N2A cells in some way, either by preventing the particles from being up-taken or changing the shape or size of the particles, then the cytotoxicity of the Cu particles are lessened on the cells. In this research, it is reasonable to suggest that any alterations in physiochemical properties after incubation with Dynasore would therefore be apparent.

It was also shown that the manufactured nanoparticles were not always in the size ranges claimed. For Cu-NP "25 nm" was measured to have an average size of 88 ± 30nm, CuO-NP "40 nm" was measured to have an average size of 78 ± 21nm, and Cu-MSP (500 nm) had an average size of 477 ± 184nm (Schrand *et al.,* In Preparation). However, for the experiments described here the original manufactured sizes will be used to designate the particles, but with the understanding that the nominal size does not represent the actual size.

3-Hydroxynaphthalene-2-carboxylic acid (3,4 dihydroxybenzylidene) hydrazide, or Dynasore, is a non-competitive inhibitor of dynamin 1, dynamin 2 and mitochondrial dynamin (Drp1) GTPase activity. Dynamin is essential for clathrin-dependent coated vesicle formation and is "required for membrane budding at a late stage during the transition from a fully formed pit to a pinched-off vesicle" while Dynasore is able to block the endocytic pathways that are dependent on dynamin and blocks vesicle formation within seconds of being added (Macia *et al*., 2006).

Figure 3-2 shows the chemical structure of Dynasore. Previous experiments showed that there was a limited increase in viability of cells that were pre-treated with Dynasore prior to NP exposure (Schrand et al, In Preparation).

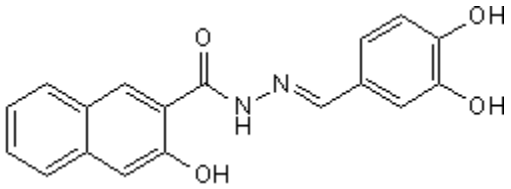

Fig 5. Chemical structure of Dynasore (Tocris Bioscience, 2010).

3.8.6 Hyperspectral Imaging (HSI) using Cytoviva®

The Hyperspectral Imaging system using Cytoviva as a light source provides a spectral analysis of nanomaterials in the visible near infrared spectral range (VNIR), from 400 to 1000 nm. While not used in this research, the HSI system can analyze for both non-fluorescent and fluorescently labeled components in live cells and nano-materials, enabling a wide range of capabilities for bio-medical research in both cell biology and infectious disease research (Cytoviva, 2011).

Hyperspectral Imaging (HSI) was conducted on control N2A cells as well as on each of the three particle types (Cu-NP 25 nm, CuO-NP 40 nm, Cu-MSP 500 nm). Copper nano and micron-sized particles scatter colored light when illuminated with white light (the Cytoviva light source). A concentric imaging spectrophotometer collects the spectra from each particle type.

Many metallic nanoparticles are able to support surface plasmons at optical frequencies. These plasmons are known as localized surface plasmons (LSPs). It is due to the recent understanding of the nature of these plasmons combined with their refractive index sensitivity that has led to using nanoparticles as biosensors (Miller and Lazarides, 2005).

When a particle is struck by an electromagnetic wave, the electrons of the particle will oscillate at the frequency of the incident wave and an oscillating electron will radiate at the same electromagnetic radiation as the oscillating electron. It is from this secondary radiation that the scattering of light occurs. Since light scattered by a particle illuminated from a monochromatic light source has the same wavelength as the incident light the distinct scattered colors coming from different particles and varying sizes can only be produced when the source (illuminating) light is a polychromatic white light. This polychromatic white light is "produced by a filament lamp operated at high color temperature" and the scattering of colors results because each type of particle will preferentially scatter light over a narrow wavelength band. Nanoparticles differing in composition, shape, size, and homogeneity as well as their medium refractive index will alter the respective particles' light-scattering properties (Yguerabide and Yguerabide, 1998).

Yguerabide and Yguerabide (1998) show that copper particles display a weak scattering band around the 380 to 550 nm region in Table 5. This can also seen in Fig 3-3, where "the light-scattering power of a particle can be expressed in terms of the light-scattering cross section" versus the various wavelengths from light scattered by various particles (Yguerabide and Yguerabide, 1998).

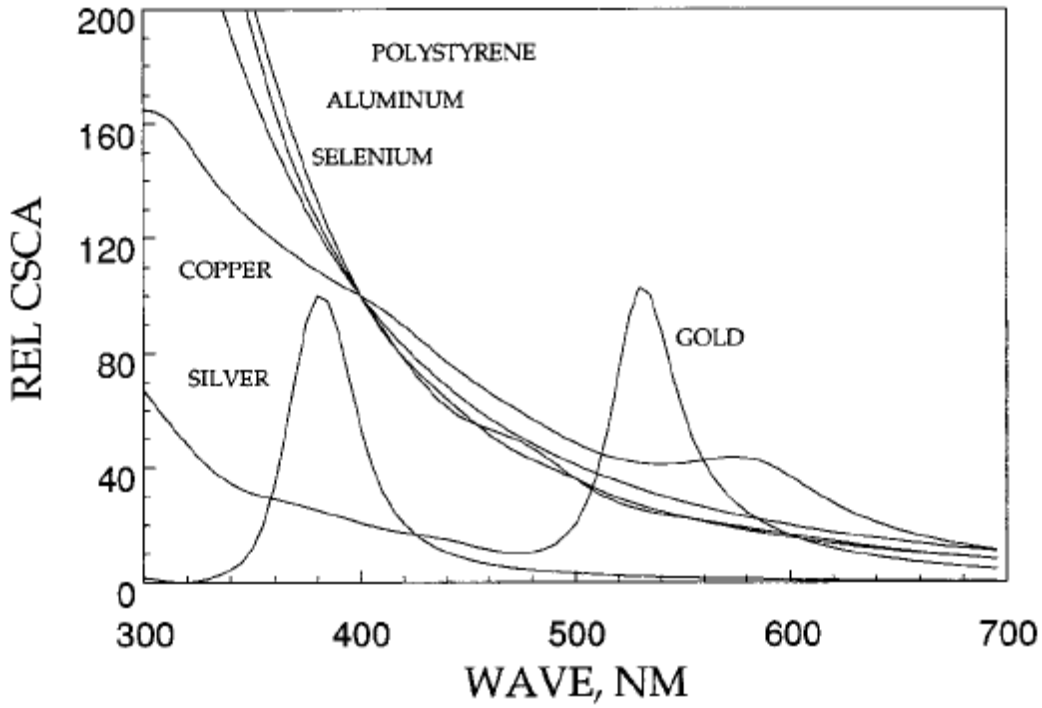

Fig 6. Graphs of light-scattering cross section vs. wavelength for various particles. (Yguerabide and Yguerabide, 1998).

Table 5. Calculated Light-Scattering and Absorption Properties for Various Particles (Yguerabide and Yguerabide, 1998).

Calculated Light-Scattering and Absorption Properties for Particles of Different Compositions (Rayleigh Scattering)

	C_{sca} (cm^2)	Wave (nm)	Rel C_{sca}	ϵ (M^{-1} cm^{-1})	φ_s
Silver	8×10^{-12}	380	1000	1.68×10^{10}	0.126
Gold	9.02×10^{-13}	530	112.7	5.88×10^{9}	0.04
Copper[a]	3.74×10^{-13}	380	46.8	2.59×10^{9}	0.038
	1.43×10^{-13}	530	17.9	1.53×10^{9}	0.025
Aluminum[a]	3.73×10^{-13}	380	46.6	2.66×10^{8}	0.369
	7.49×10^{-14}	530	9.36	8.77×10^{7}	0.225
Selenium[a]	1.85×10^{-13}	380	23.1	5.41×10^{8}	0.09
	3.69×10^{-14}	530	4.61	1.69×10^{8}	0.057
Polystyrene[a]	3.76×10^{-15}	380	0.47	9.88×10^{5}	1
	9.93×10^{-16}	530	0.124	2.61×10^{5}	1

Note. Values given in the table were calculated with the Rayleigh equation. Particle diameter = 30 nm. Medium refractive index = 1.33. C_{sca} = scattering cross section at specified wavelength; Wave = wavelength; Rel C_{sca} = scattering cross section divided by scattering cross section of silver at 380 nm and multiplied by 1000. ϵ = Molar decadic extinction coefficient = 2.63×10^{20} C_{ext}. φ_s = Light scattering yield = $C_{sca}/(C_{sca} + C_{abs})$.

[a] This particle does not have a prominent light-scattering or absorption peak in the visible region of the spectrum. The cross sections decrease continuously with increasing wavelength. Data are arbitrarily tabulated at the wavelengths shown in the table.

3.9 Statistical Analysis

Statistical Analysis was performed for the MTS data as mean ± standard deviation.

IV. Data Description and Analysis

4.1 Introduction

This Chapter presents the data gathered from the methodologies described in Chapter 3. The chapter includes, in this order: 24 hour exposure MTS data of N2A to Cu-NPs, Cu-MSPs and CuO-NPs, and $CuCl_2$, DLS experimental data, LVEM images, ESEM images, SEM images, TEM images at various time-points and HSI with Cytoviva.

4.2 MTS data

MTS was performed on the three types of Cu particles and $CuCl_2$. The results of This cellular proliferation assay can be seen in Fig 4-1.

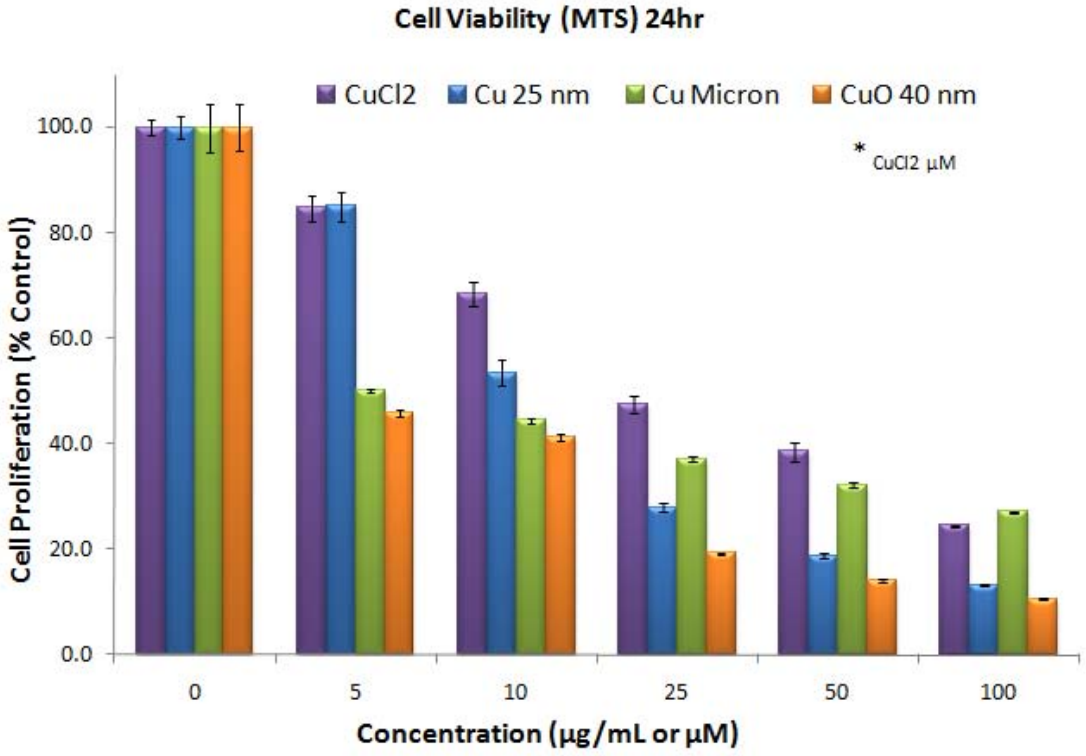

Fig 7. MTS assay for the three types of Cu particles and $CuCl_2$. (Concentration in µg/mL for NPs and µM for $CuCl_2$)

In terms of cellular viability, $CuCl_2$ is the least toxic at all concentrations. Cu-NP 25 nm is less toxic at low concentrations (< 25 μg/mL) than Cu-MSP 500 nm and CuO-NP 40 nm. At concentrations above 25 μg/mL, Cu-NP 25 nm becomes comparable in toxicity to CuO-NP 40 nm and more toxic than Cu-MSP 500 nm. From further characterization, it is not surprising that the Cu-NP 25 nm and CuO-NP 40 nm share similar toxicities. As these two particles become suspended in water for longer periods of time, they both become oxidize, especially Cu-NP 25 nm, which may explain the similarities in toxicities.

4.3 Dynamic Light Scattering Experiments

Dynamic Light Scattering Experiments were conducted in order to observe changes in the dynamic size of Cu-NPs, CuO-NP, and Cu-MSP under cell culture conditions. An initial trial of DLS was conducted for the particles at 50 μg/mL concentration with dosing media. The general conclusion is that at these conditions there is a trend for the Cu particle sizes to increase. The surprising aspect of size observation in solution is that it follows an inverse trend compared to the primary size of the particles: CuO-NPs > Cu-NPs > Cu-MSPs (Schrand *et al.*, In Preparation).

Previous studies show limited cellular modulation with co-incubation with Dynasore. An initial experiment was conducted to serve as a control for change in particle agglomeration for the Cu-NP (25 nm), CuO-NP (40 nm), and Cu-MSP (500 nm) with 3, 6, and 24 hour incubation times without the use of the endocytosis inhibitor Dynasore. Cu particles were freshly diluted from 1 mg/mL stock solutions prior to readings. Table 6 shows concentration and incubation times. In general agglomerations

became larger as incubation time increased from 3 to 24 hours with the exception of the Cu-NP 25 nm. Dynamic sizes of the particles under cell culture conditions are CuO-NPs > Cu-MSPs > Cu-NPs, which is similar to the sizes measured earlier by Schrand *et al*.

Table 6. Concentration and incubation times used for DLS control experiment without Dynasore

Sample & concentration	Cu particle volume, dosing media volume	0 hour incubation	3 hour incubation	24 hour incubation
Cu-NP (25 nm) 25 µg/mL	25 µg/mL Cu 975 µL dosing media	0 hour incubation	3 hour incubation	24 hour incubation
CuO-NP (40 nm) 25 µg/mL	25 µg/mL Cu 975 µL dosing media	0 hour incubation	3 hour incubation	24 hour incubation
Cu-MSP (500 nm) 25 µg/mL	25 µg/mL Cu 975 µL dosing media	0 hour incubation	3 hour incubation	24 hour incubation

Figures 8A, 6B, and 6C show the results of this initial DLS experiment.

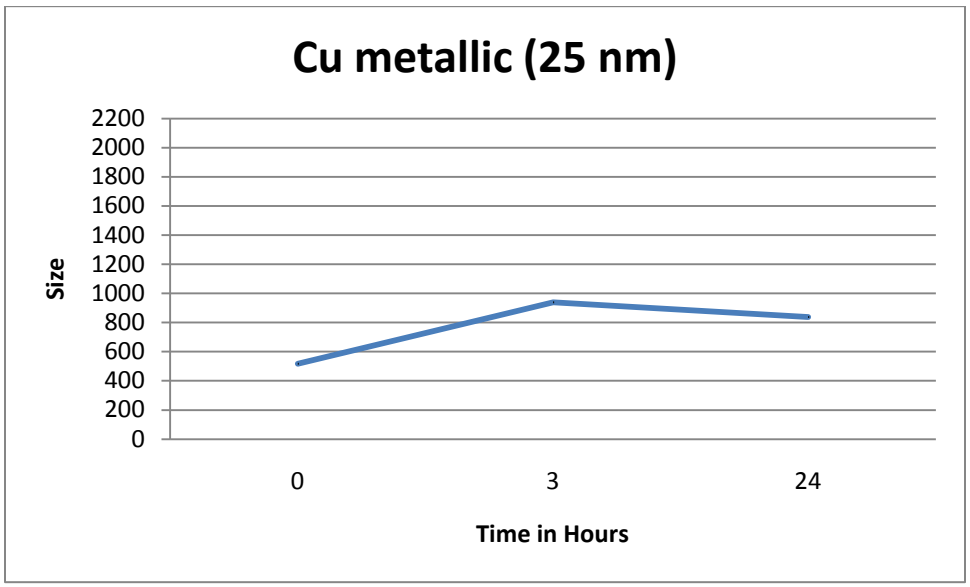

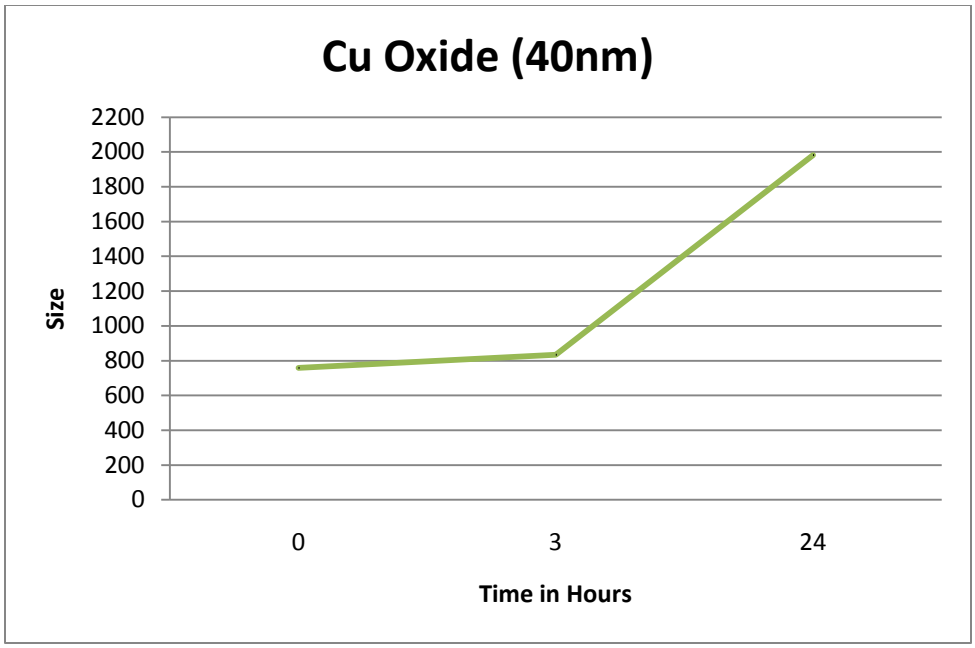
Cu Oxide (40nm)
2200
2000
1800
1600
1400
1200
1000
800
600
400
200
0
Size
0
3
24
Time in Hours

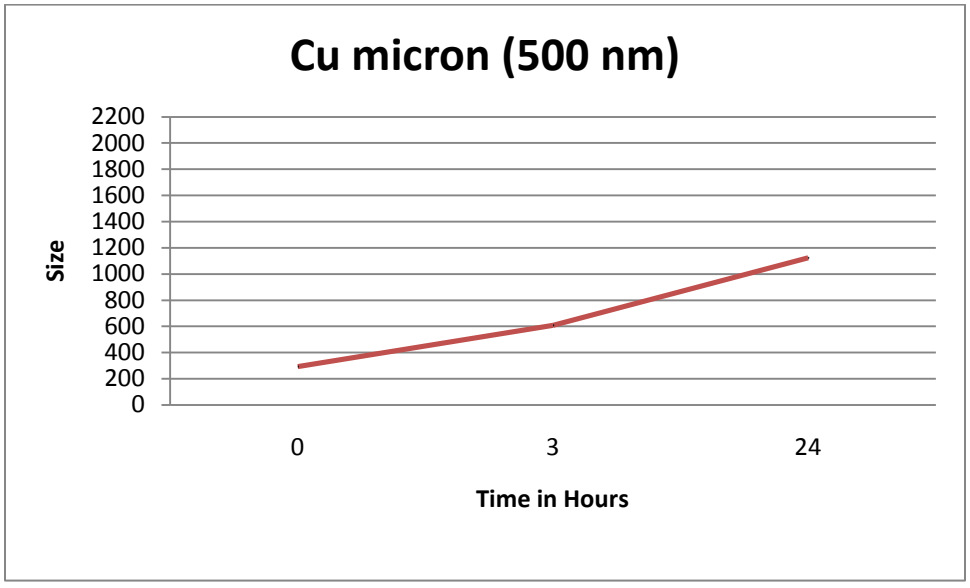
Cu micron (500 nm)
2200
2000
1800
1600
1400
1200
1000
800
600
400
200
0
Size
0
3
24
Time in Hours

The next set of DLS experiments involve three trials of Cu-NP, CuO-NP, and Cu-MSP in dosing media at three different concentrations of 25 µg/mL, 50 µg/mL, and 100 µg/mL as seen in Table 7. Measurements were taken at 0 and 3 hours for each particle at each concentration. 25 µM of the endocytosis inhibitor Dynasore was also added to each sample because ultimately the goal is to understand if the chemical has any effect on the viability of the N2A cells as seen in previous studies.

Table 7. Cu particle, Dynasore and dosing media volumes

Final concentration for samples	Cu particle volume	Dynasore volume	Dosing Media	Total Volume
25 µg/mL Cu particle + 25 µM Dynasore	25 µL	25 µL	950 µL	1000 µL
50 µg/mL Cu particle + 25 µM Dynasore	50 µL	25 µL	925 µL	1000 µL
100 µg/mL Cu particle + 25 µM Dynasore	100 µL	25 µL	875 µL	1000 µL

Figures 9A through 9I show size distributions from this DLS experiment.

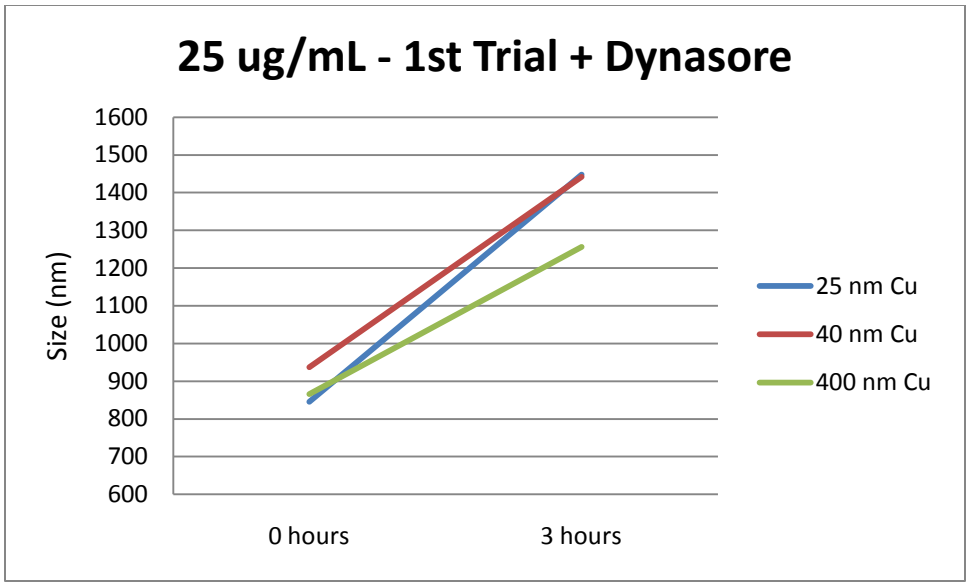

Fig 9A. Size distribution of Cu particles at a concentration of 25 µg/mL and Dynasore at both 0 and 3 hours of incubation, 1st trial

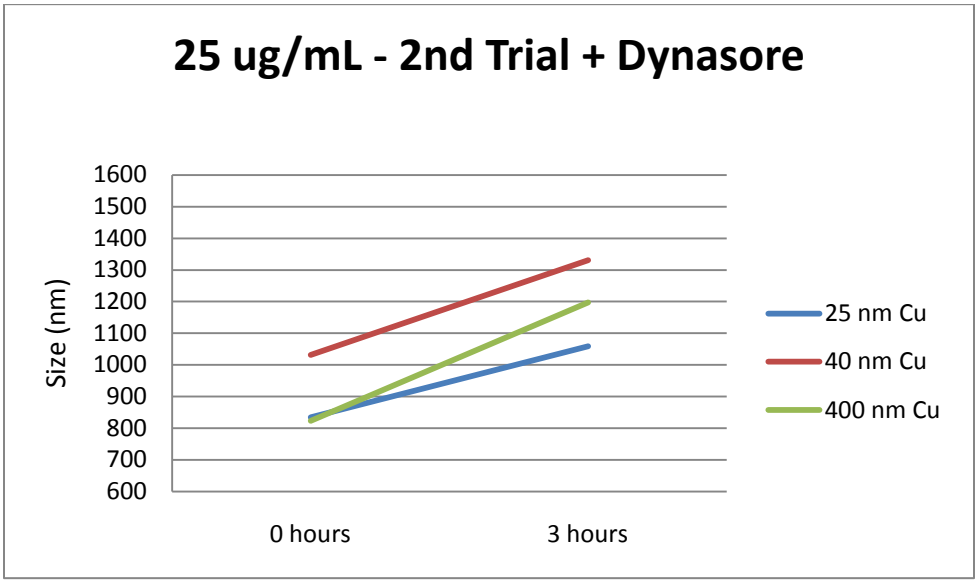

Fig 9B. Size distribution of Cu particles at a concentration of 25 µg/mL and Dynasore at both 0 and 3 hours of incubation, 2nd trial

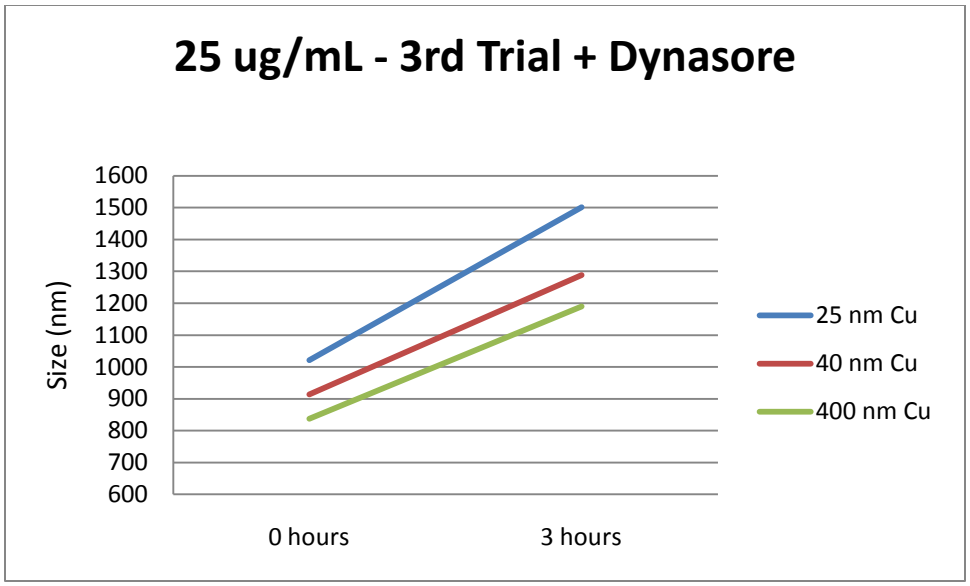

Fig 9C. Size distribution of Cu particles at a concentration of 25 µg/mL and Dynasore at both 0 and 3 hours of incubation, 3rd trial

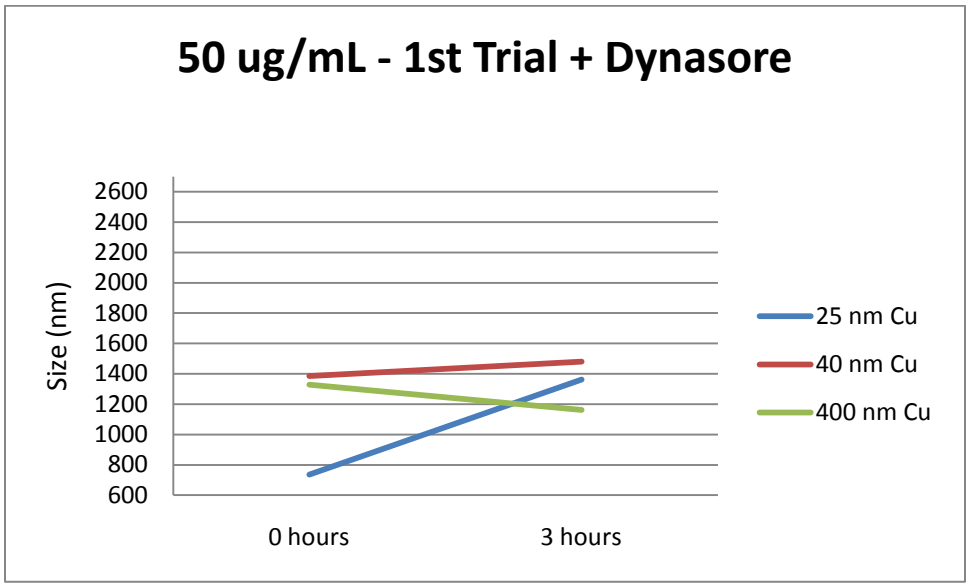

Fig 9D. Size distribution of Cu particles at a concentration of 50 µg/mL and Dynasore at both 0 and 3 hours of incubation, 1st trial

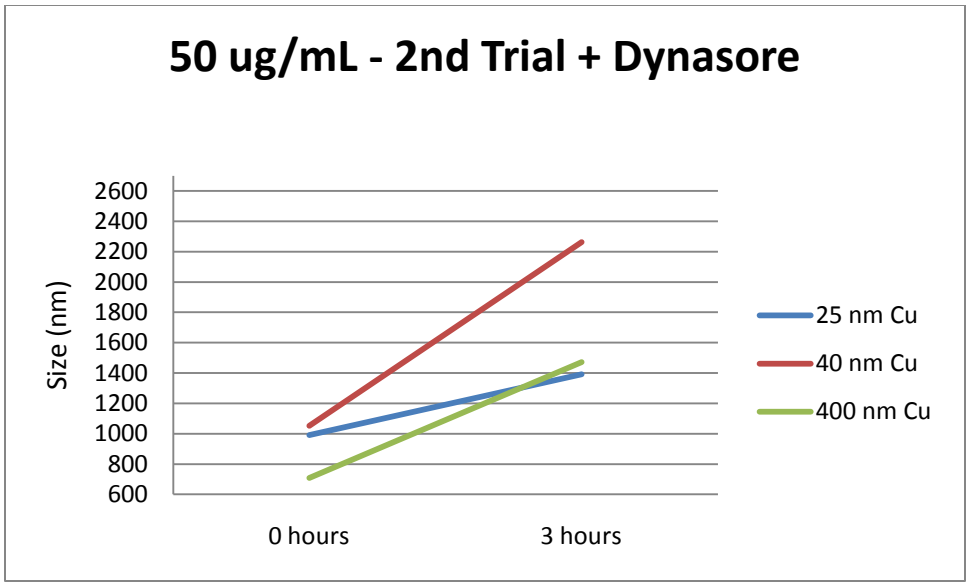

Fig 9E. Size distribution of Cu particles at a concentration of 50 µg/mL and Dynasore at both 0 and 3 hours of incubation,2nd trial

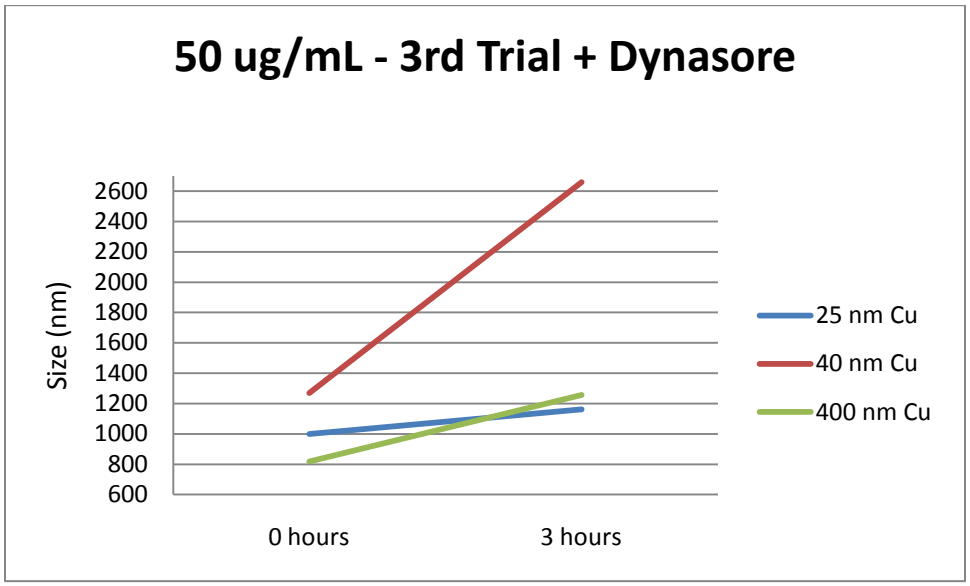

Fig 9F. Size distribution of Cu particles at a concentration of 50 µg/mL and Dynasore at both 0 and 3 hours of incubation, 3rd trial

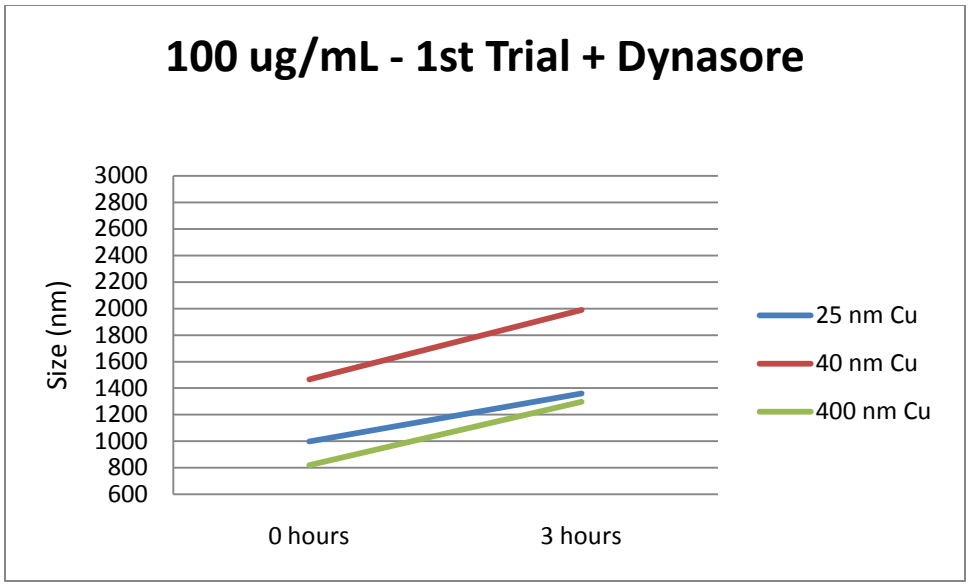

Fig 9G. Size distribution of Cu particles at a concentration of 100 µg/mL and Dynasore at both 0 and 3 hours of incubation, 1st trial

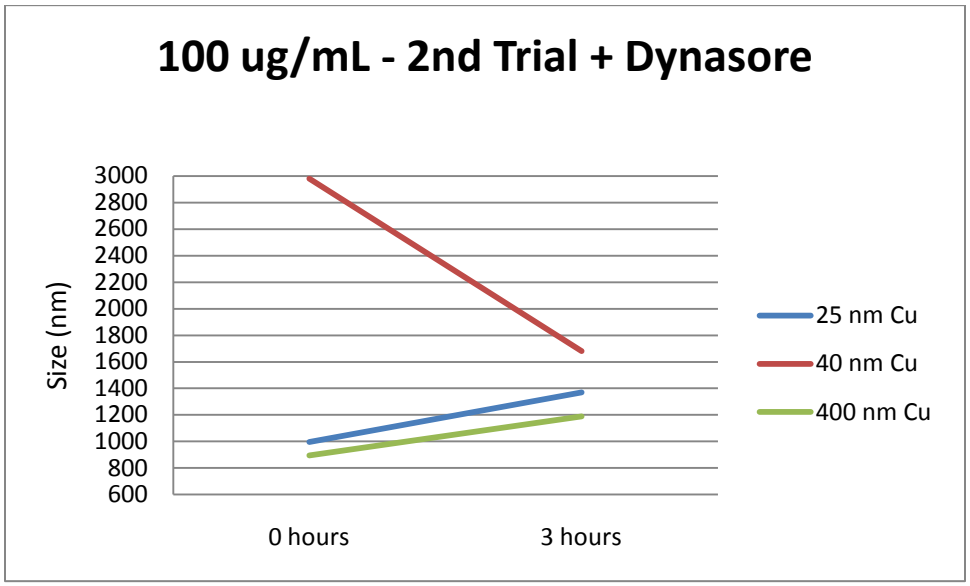

Fig 9H. Size distribution of Cu particles at a concentration of 100 µg/mL and Dynasore at both 0 and 3 hours of incubation, 2nd trial

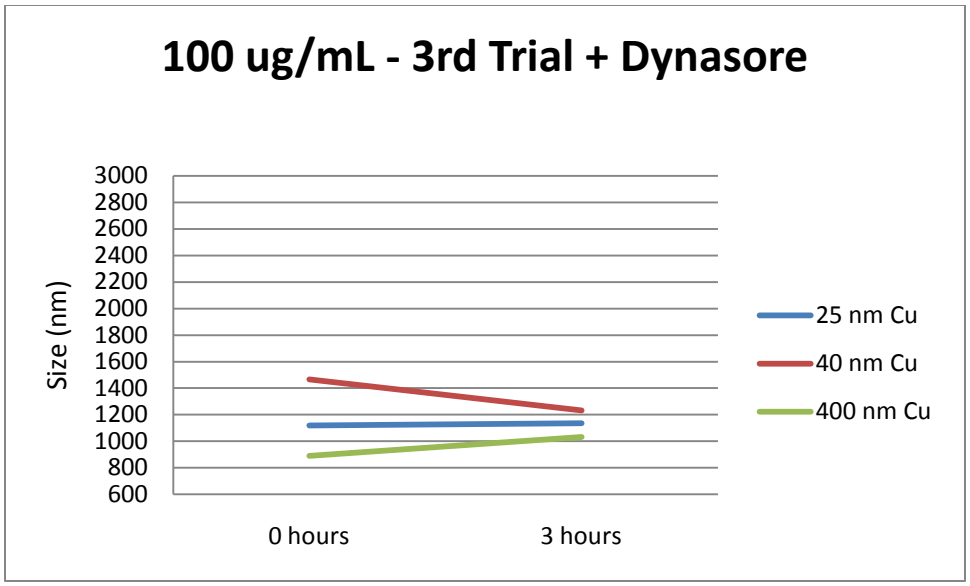

Fig 9I. Size distribution of Cu particles at a concentration of 100 µg/mL and Dynasore at both 0 and 3 hours of incubation, 3rd trial

4.4 LVEM Imaging

In Fig 10 A-C, LVEM images of the three particles are shown. The LVEM may not produce the sharpest images but the process is not time consuming or difficult to set up. From these images basic particle morphology and agglomeration behavior can be observed.

Fig 10A. Cu-NP 25 nm at 202 kx magnification

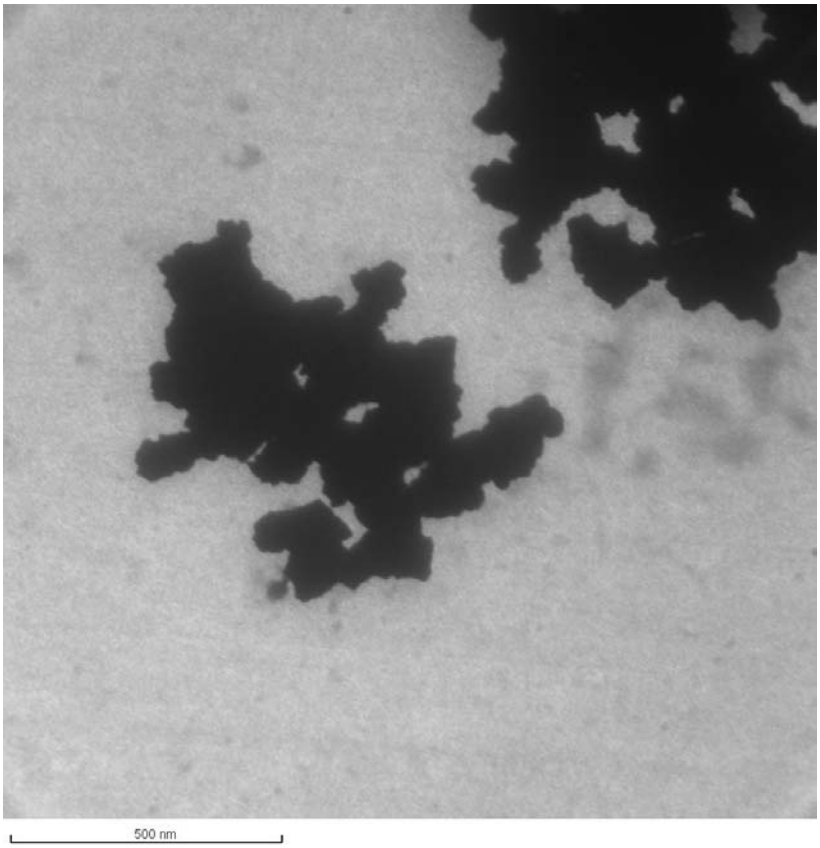

Fig 10B. CuO-NP 40 nm at 202 kx magnification

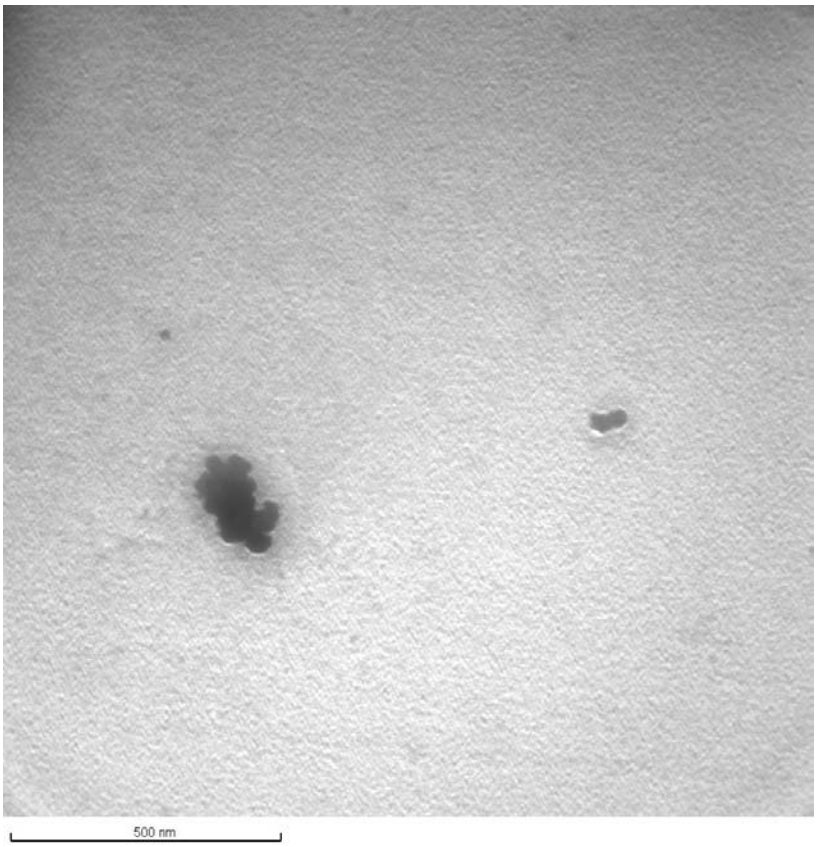

Fig 10C. Cu-MSP 500 nm at 202 kx magnification

4.5 ESEM Imaging

Environmental Scanning Electron Microscopy was conducted on Cu-NPs, CuO-NPs, and Cu-MSPs 3 months after suspension in water. The particles were diluted from stock solutions and the goal of the microscopy was to aid in the characterization of the physiochemical properties of the particles themselves. Examination of surface roughness is an indicator of the amount of oxidization the particles experience and may elucidate particle uptake sizes. Figures 11A-B illustrate the original images captured.

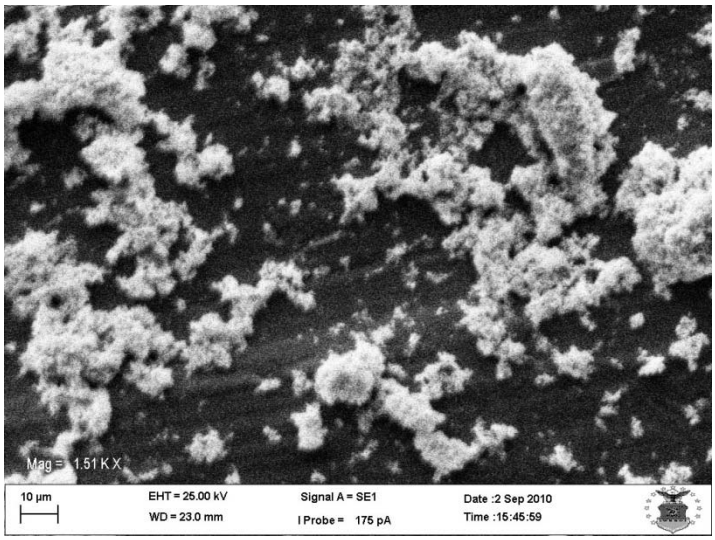

Fig 11A. Cu-NP 25 nm at 3 months

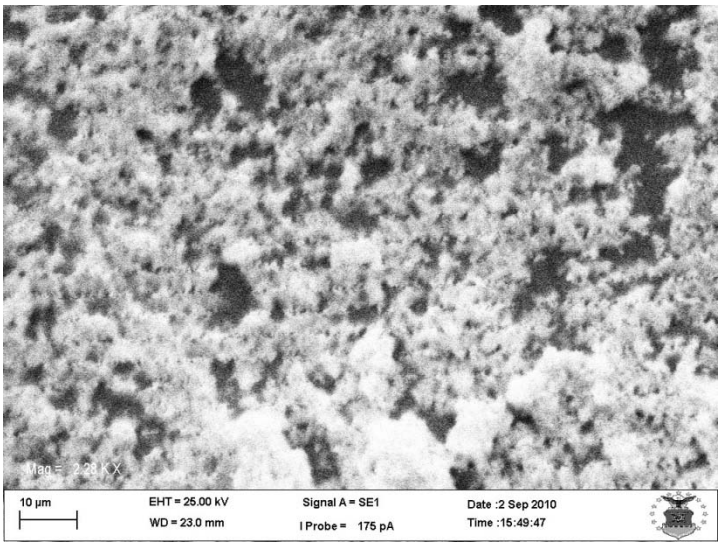

Fig 11B. CuO-NP 40 nm at 3 months

4.6 SEM Imaging

SEM images were taken after N2A cells were dosed with Cu particles in an experiment to visually determine the placement of particles and cells in dosing media. All particles were dosed at a concentration of 25 μg/mL. Fig 12A-D show a series of images including a control image and that of the three particles.

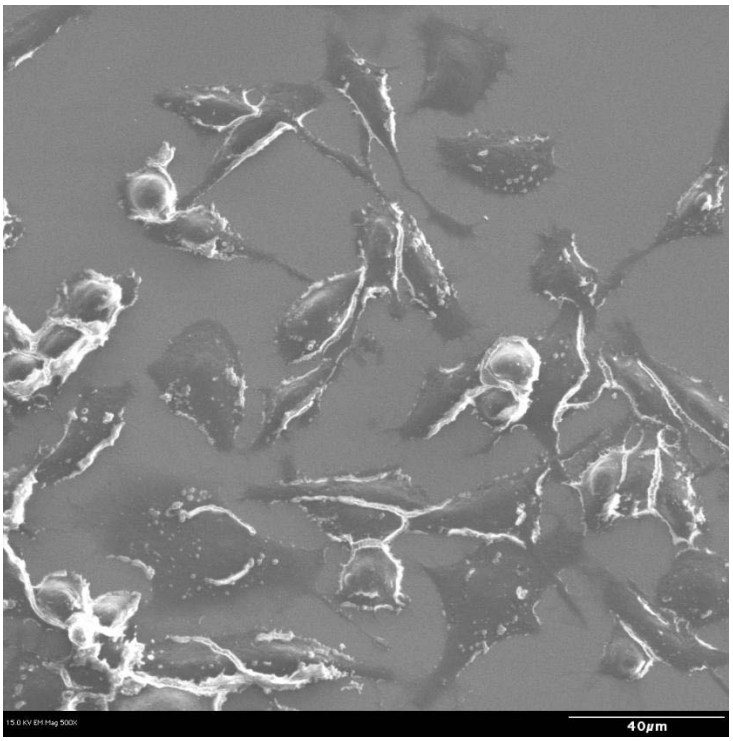

Fig 12A. Control image without Cu-NPs
(Image taken by Dr. Amanda Schrand)

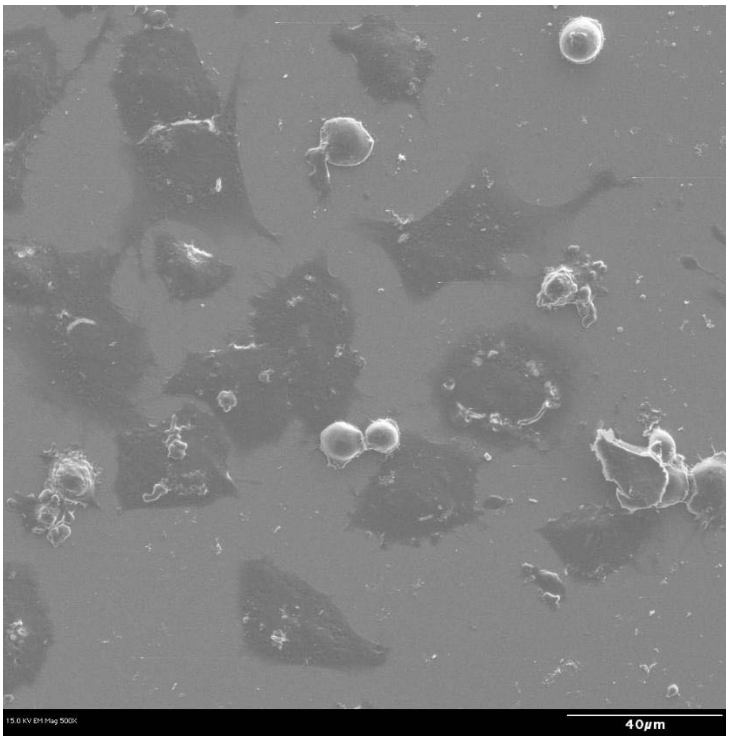

Fig 12B. Cu-NP 25 nm
(Image taken by Dr. Amanda Schrand)

Although some charging is seen in the image, the Cu-NP 25 nm can be seen fairly clearly with the N2A cells showing up as darker shadowy figures. In scanning electron microscopy, charging effects are described where excess negative charge accumulates on the specimens and image artifacts arise from excess surface charge and produce poor images. At times it may be necessary to prepare poorly conducting specimens with a metallic coating such as gold (Shaffner and Van Veld, 1971).

The control image shows the cells without any Cu NP dosing, and the cells are observed be more adherent and neuron like with more dendrites present. As the N2A cells are dosed with the Cu particles they are under more oxidative stress and thus start to become rounder and less adherent to the glass cover-slip surfaces.

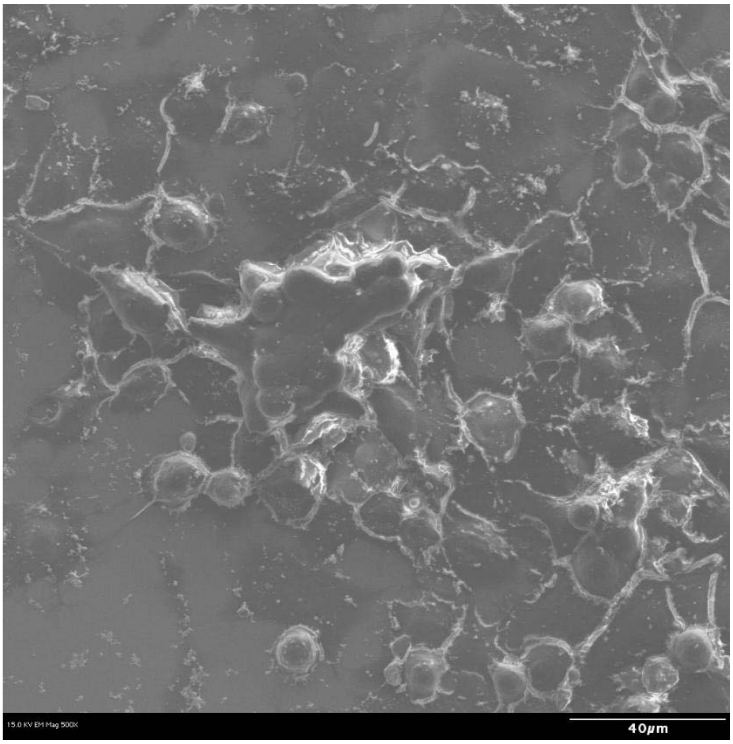

Fig 12C. CuO-NP 40 nm
(Image taken by Dr. Amanda Schrand)

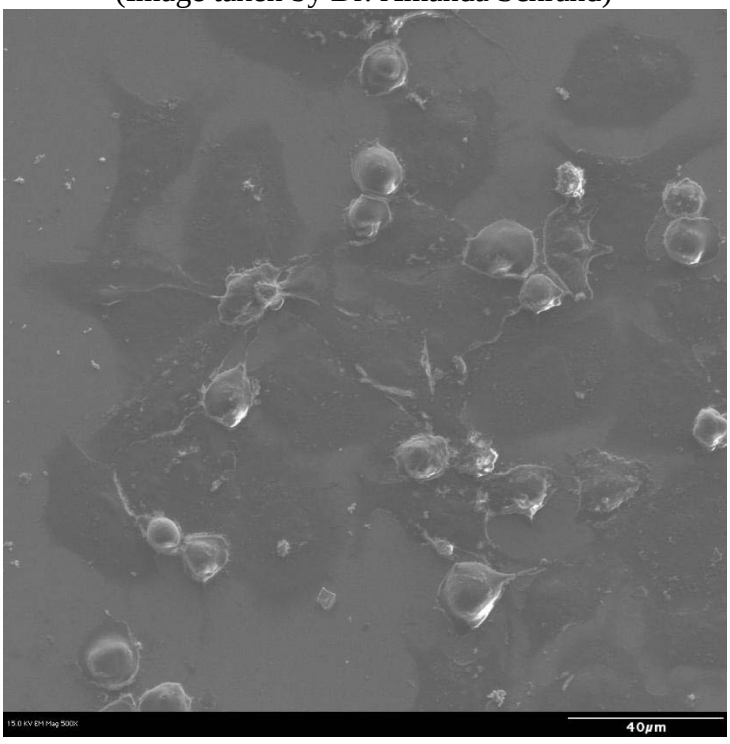

Fig 12D. Cu-MSP 500 nm

(Image taken by Dr. Amanda Schrand)

4.7 TEM Imaging

TEM Imaging was conducted on the Philips Lab 6 TEM at the AFRL Materials Laboratory. The following figures show the morphology and sizes of the particles suspended in water: initially after preparation, at 2 or 3 months after preparation, and again at 6 months. The surface oxidation, agglomeration, and sizes indicate changes the particles experience over time.

It is worth noting that initial TEM imaging was conducted along with a brief study on the size distribution of the particles. Interestingly, as was also found in the study by Schrand *et al.* (In Preparation) referred to earlier, the Cu-NP 25 nm has a larger average size than the CuO-NP 40 nm. This is important to realize; nominal sizes provided by the manufacturer may not be indicative of the true particle size. The stock particles, in powder form, are preserved under Argon gas, but even so, properties of the particles may change over time.

The three different types of particles were imaged again after 2 or 3 months to look for any changes in oxidation, morphology, and overall surface properties. Fig 13A-C show images of the three types of particles.

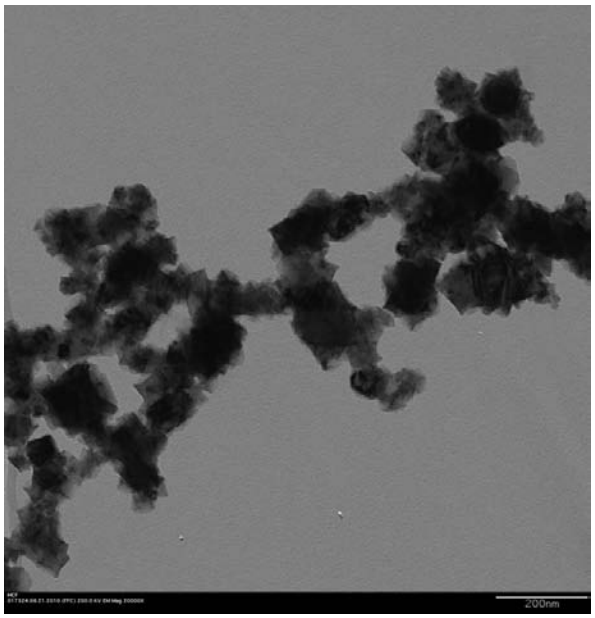

Fig 13A. Cu-NP 25 nm at 2 months

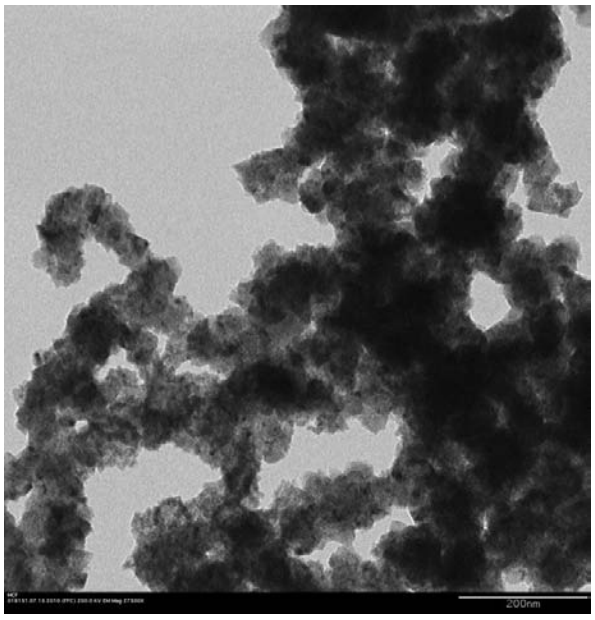

Fig 13B. CuO-NP 40 nm at 3 months

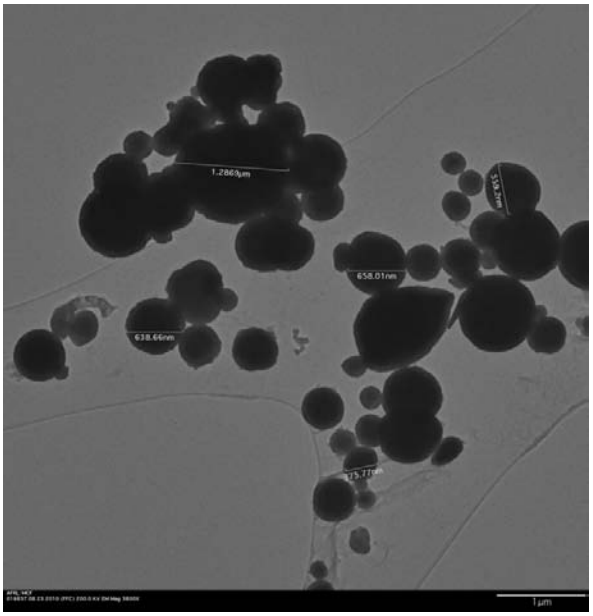

Fig 13C. CuO-MSP 500 nm at 3 months

Figures 14, 15, and 16 show the comparison images of the three particles at 6 months. Comparison images were taken at standard magnifications of 3800x, 8800x, 15000x, 50,000x, and 80,000x so improved observations can be made.

Fig 14. Cu-NP 25 nm at 6 months

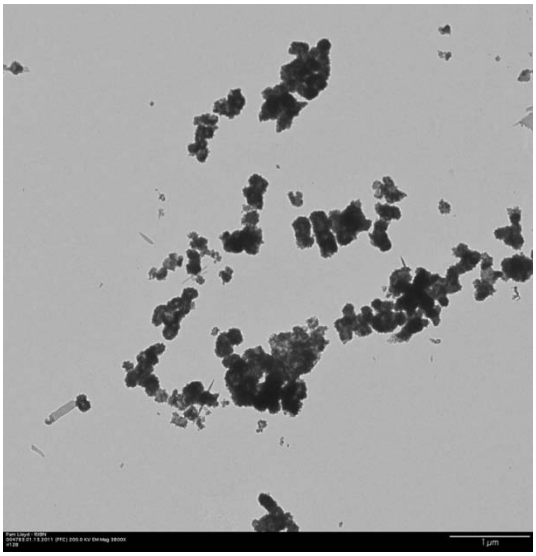

Fig 14A. 3800x

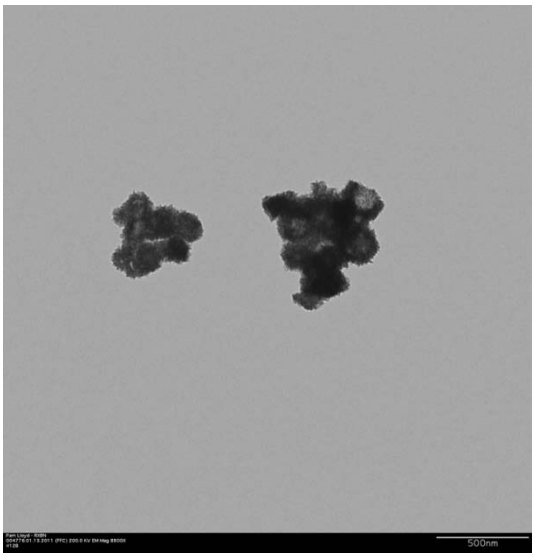

Fig 14B. 8800x

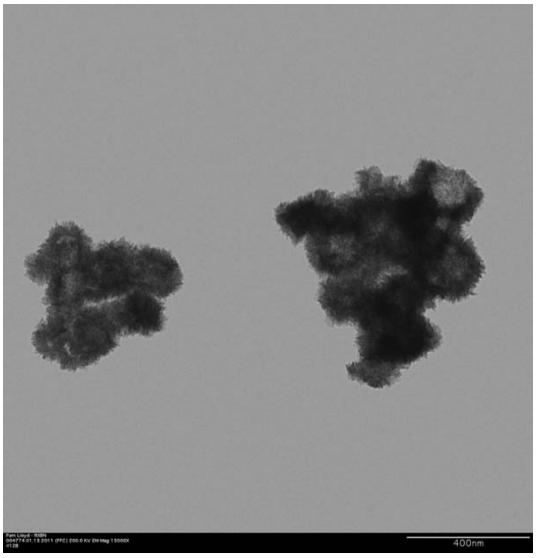

Fig 14C. 15,000x

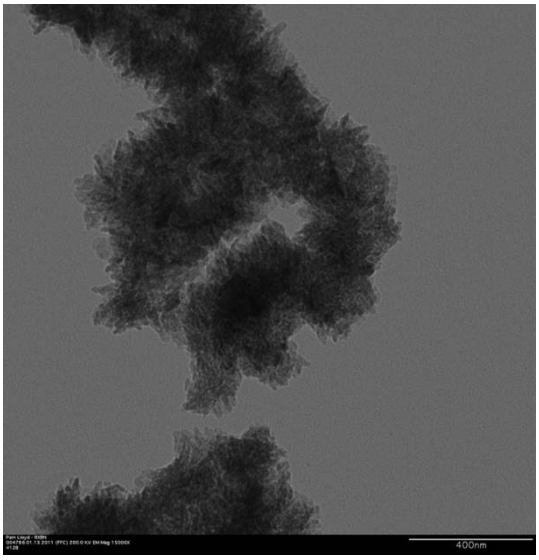

Fig 14D. 50,000x

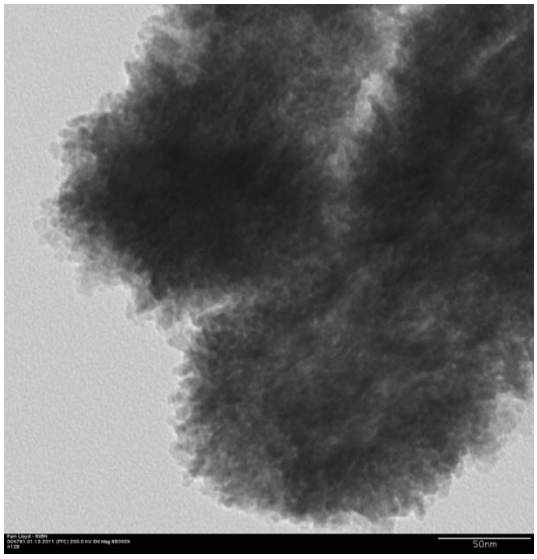

Fig 14E. 80,000x

Fig 15. CuO-NP 40 nm at 6 months

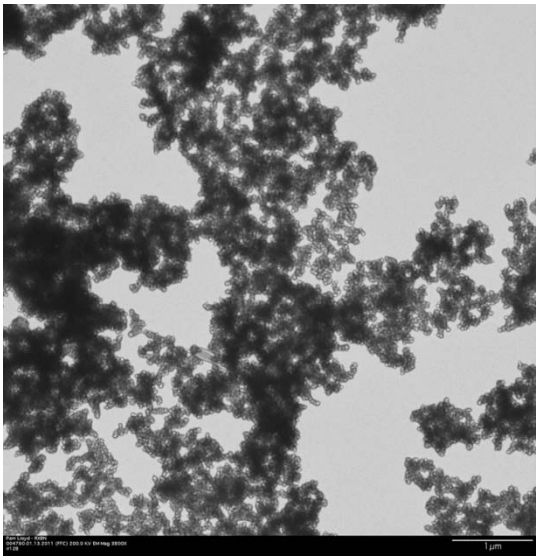

Fig 15A. 3800x

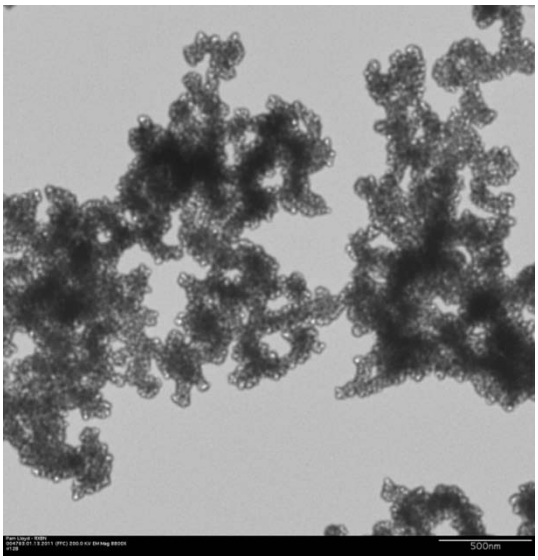

Fig 15B. 8800x

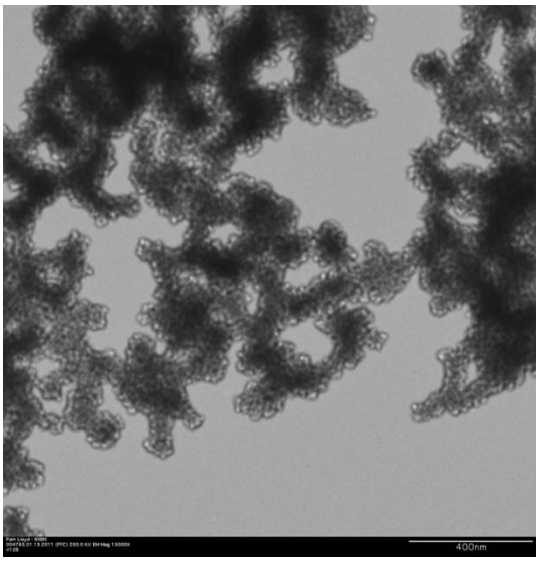

Fig 15C. 15,000x

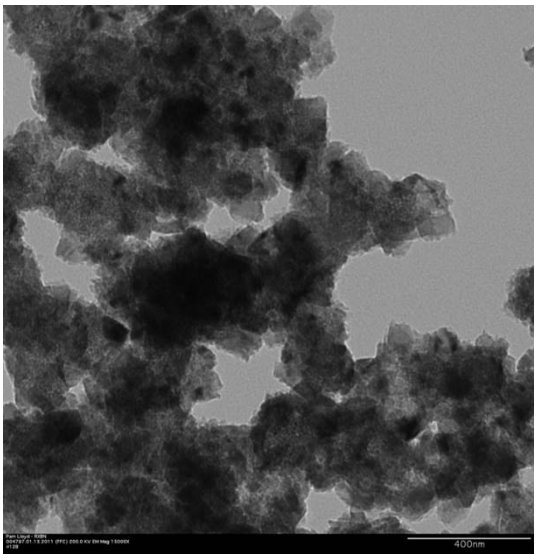

Fig 15D. 50,000x

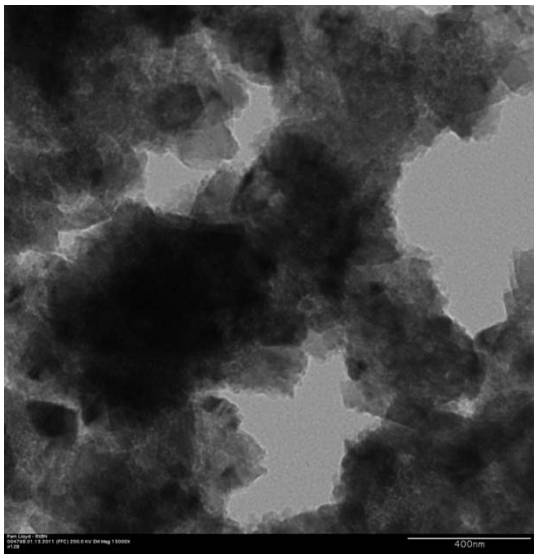

Fig 15E. 80,000x

Fig 16. Cu-MSP 500 nm at 6 months

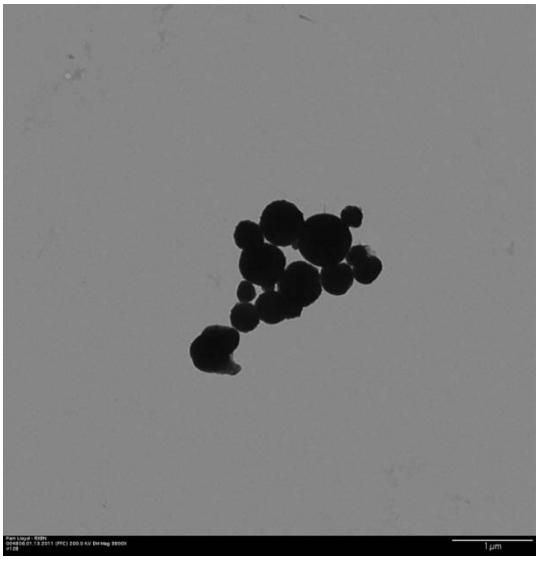

Fig 16A. 3800x

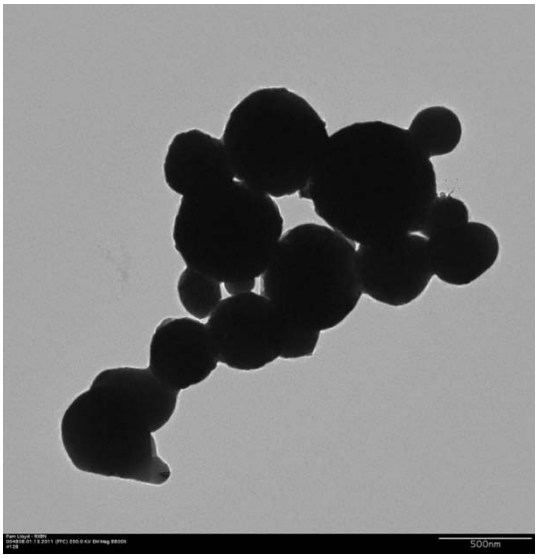

Fig 16B. 8800x

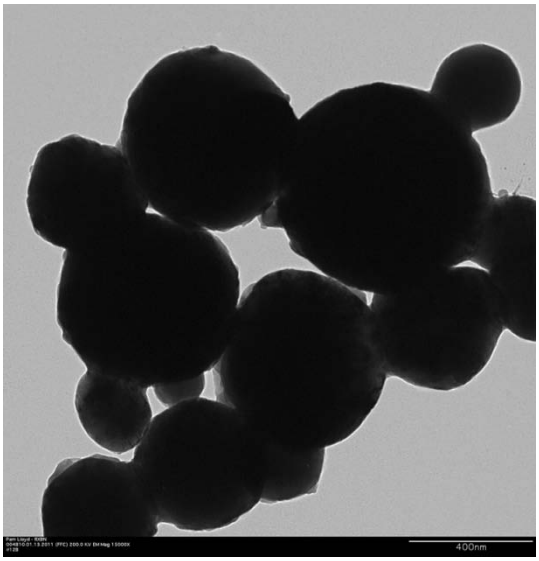

Fig 16C. 15,000x

Fig 16D. 50,000x

Fig 16E. 80,000x

4.8 Hyperspectral Imaging

Hyperspectral Images and spectra.

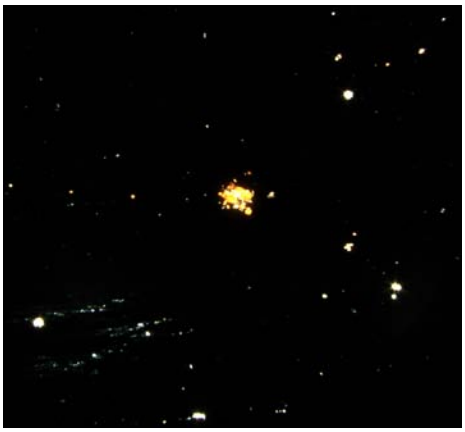

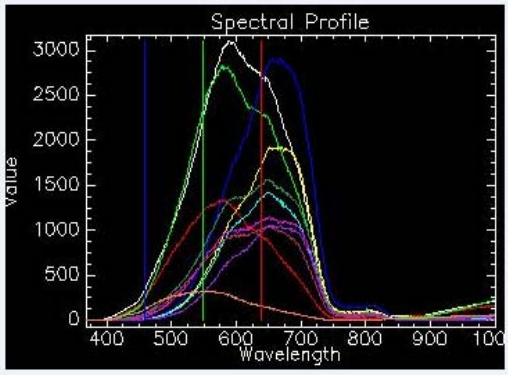

Fig 17A. HSI image of Cu-NP 25 nm with Spectral Profile.

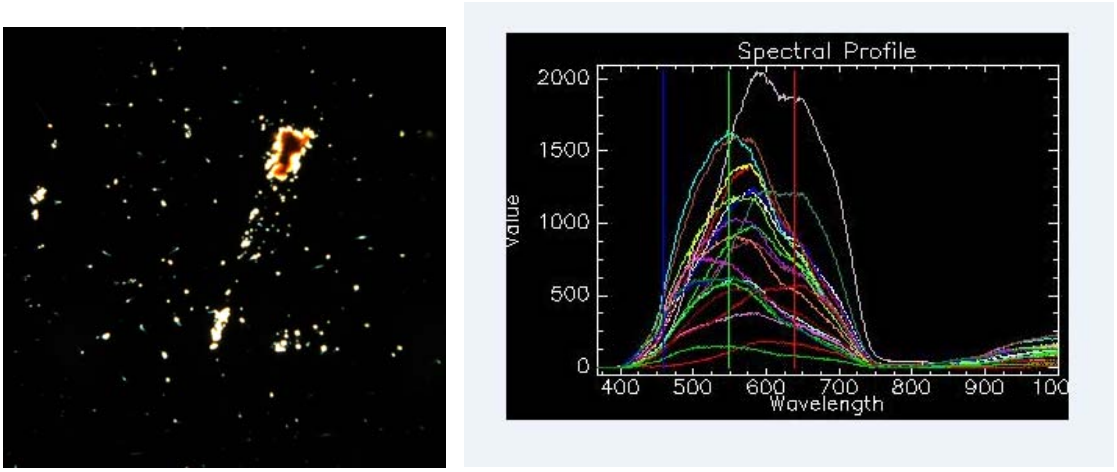

Fig 17B. HSI image of CuO-NP 40 nm with Spectral Profile

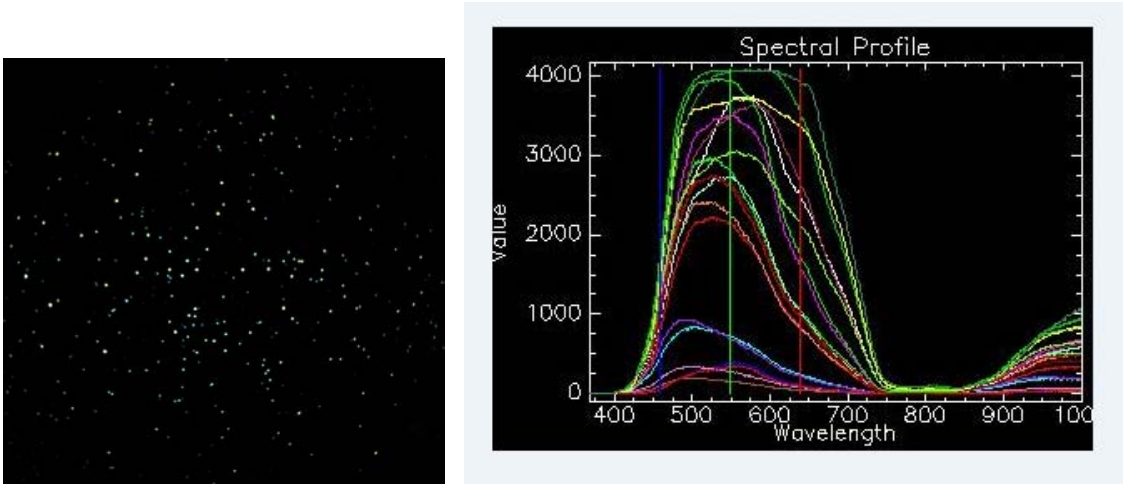

Fig 17C. HSI image of Cu-MSP 500 nm with Spectral Profile

Unfortunately, it was also shown that copper does not have a “prominent light-scattering or absorption peak in the visible region of the spectrum” (Yguerabide and Yguerabide, 1998). This makes it very difficult to draw any conclusions from the HSI data as there is not a clear plasmonic peak for copper and the collected spectra of

dissimilar sizes of copper nano and micron-sized particles would not give much information.

Careful inspection of the three spectral profiles shows that there are very broad peaks and it is difficult to pinpoint any specific peaks. From chapter 3, Yguerabide and Yguerabide (1998) show that the copper band should fall somewhere between 380-530 nanometers, yet these spectra show broad bands between 500-800 nanometers. This could be due to agglomeration of the particles but regrettably no additional information is provided such as oxide content between the various particles as no clear “shift” can be observed.

V. Conclusions and Future Research Considerations

5.1 Overview

This chapter summarizes the results of this research and suggests additional studies that may aid to further characterize Cu-NPs, Cu-MSPs and CuO-NPs. Suggestions for methodology improvements are discussed as well as further additional research that may aid in better characterization.

5.2 Conclusions

This research compared the effects upon N2A cellular viability by the three types of Cu particles and characterized these particles using a variety of techniques. Toxicity changed for the N2A cells at different concentrations and for different particles. At high concentrations, N2A cells fared better when dosed with Cu-MSP 500 nm. This may be related to cellular mechanisms where cellular uptake is generally limited for large particles around 500 nm, thus enabling smaller Cu particles to be uptaken easier. Characterization showed a general increase in size when the particles were incubated with the endocytosis inhibitor Dynasore. This may also explain apparent "rescue" effects seen in previous research, where there was increased cellular viability in the presence of Dynasore. At higher concentrations of particles (100 μg/mL) with 25 μM Dynasore trends are somewhat more inconclusive, suggesting possible interferences in the solution or between the particles themselves as far as forming agglomerations.

Additionally, this research seeks to observe *in vitro* effects upon murine neuroblastoma cells (N2A) by these three types of particles as well as by $CuCl_2$. Microscopy techniques indicate observable changes in oxidation for Cu-NP 25 nm and

CuO-NP 40 nm after suspension in water over long incubation. In general, agglomerations of the particles increase when dosed with the endocytosis inhibitor Dynasore. In terms of cellular viability, $CuCl_2$ is the least toxic at all concentrations. Cu-NP 25 nm is less toxic at low concentrations (< 25 μg/mL) than Cu-MSP 500 nm and CuO-NP 40 nm. At concentrations above 25 μg/mL, Cu-NP 25 nm becomes comparable in toxicity to CuO-NP 40 nm and more toxic than Cu-MSP 500 nm.

5.2.1 Imaging

Various techniques for imaging cells and toxicity studies were conducted with the nano and micron-sized particles. A general rough estimate of sizes and morphology was conducted with the LVEM. More detailed imaging was conducted with the ESEM and SEM. Finally the high resolution TEM was used to look at changes in surface morphology, oxidation and size over time. DLS was also used to estimate the agglomeration of the particles while dark field microscopy with Cytoviva as a light source provided insight on particle uptake and provided particle spectral profiles. Each of these techniques was useful in directing the focus of this research and providing insights, but each technique also had its own limitations.

The ESEM imaging, though not very successful, was used to gain more information on general particle morphology. Image quality and instrument availability was problematic, but a few images did show likely nanoparticle agglomerations on the surface of the ESEM stub. Additional technique modifications with ESEM may be helpful for future research. SEM imaging with the cells gave good morphological indications of healthy cells as more rounded than those receiving increasing doses of Cu

particles and proved qualitatively that the technique worked well. TEM imaging, though the most time consuming and very difficult to schedule for, was critical in determining particle morphology and had the best results. Previous studies show very low, if any Cu particle uptake into N2A cells and future studies may be needed in order to determine particle locations in respect to the N2A cells and overall changes in N2A morphology after Cu particle exposures (Schrand, In Preparation).

5.3 Recommended Additional Research

5.3.1 Characterization and Exposure

Characterization may have been affected by other experimental conditions that may have interfered with the results. Vortexing of the particles was consistent prior to dosing or experimentation, but sonication of the particles was not. Sonication of particles may have immense effects on their properties so sonication should be conducted more carefully and consistently in the future.

Other techniques that are emerging such as the separation of the Cu metal and the Cu ions can prove to be helpful in determining whether the cellular toxicity is due to the actual metal or the corresponding ions. This will also enable other techniques to determine the quantity of Cu that is released into the cell medium for exposure studies.

More repetitions on the DLS can be conducted to try to find better trends in particle agglomeration sizes and behaviors in solution. The endocytosis inhibitor Dynasore previously demonstrated to increase cellular viability is still inconclusive and need to be further explored as to exactly what are the potential mechanisms for reducing cytotoxicity for N2A cells.

Appendix A: General Maintenance and Toxicity Testing of N2A Cell Line (Schrand & Hussain, 2005)

PURPOSE/PRINCIPLE: This standard operating procedure describes the *in vitro* methods for maintaining N2A (neuroblastoma cells) for toxicity testing procedures including formulations for MTS.

KEY WORDS: N2A, neuroblastoma, cell culture, *in vitro*, nanotoxicity.

1. SAFETY AND OPERATING PRECAUTIONS:

1.1 Practice aseptic technique and work with all cells and solutions under the biological hood.

1.2 Wear appropriate gloves, eye goggles and lab coat when handling hazardous materials.

1.3 Properly dispose of unused/spent toxic materials (nanoparticles).

2. EQUIPMENT/MATERIALS/REAGENTS:

2.1 Culture media (DMEM/F12 (Sigma powder), 10% fetal bovine serum (FBS), and 1% antibiotics (Pen/Strep)

*Note: discard if pink (too acidic) or orange (too basic)…should be red/orange in color

2.2 Flasks, plates, slides for growing cells

2.3 Trypsin for detaching adherent cells

2.4 Acidified IPA with 70% isopropanol for dissolving cells

300mL 70% IPA and 1.64mL conc. HCl

2.5 MTS ($C_{18}H_{16}N_5SBr$, Cat#M2128 Sigma)

200 mg MTS (in freezer, Rm 169), 40ml PBS, mix on stir plate for ~15 minutes, store covered in foil due to light sensitivity, dated, good for 2-4 weeks

2.6 Nanomaterials with a known concentration typically diluted in water for a stock solution of concentration 1-10 mg/ml

2.7 Olympus IX71 Inverted Microscope with 12 bit QICAM from IMAGINE (Lab 160)

SPECIMEN/SAMPLE: Seed cells at high enough density to achieve 80% confluency by time of treatment. For example, if you are seeding on Friday and want to treat on Monday (3 days of growth time), seed at 200-300K cells/mL. If you are seeding on Monday and want to treat on Tuesday (24h of growth time), seed at 500-600+ K cells/mL. For better imaging conditions of individual cells, seed at 100-250K cells in 1 mL of culture media.

*Note: Check cells before dosing to optimized for your cells. If you are performing an MTS assay and you expose them before they are confluent, your "intensity" of blue color will be very low and you won't get readings. The more cells you have, the more "blue" will develop/stronger your "signal."

3. PASSAGING CELLS

4.1 Use 1-2 mls of 1% trypsin to release cells from the bottom of cell culture flasks. Avoid tapping if clumps form.

*Note: N2A cells are a mixture of floating and adherent cells

4.2 Add 5-10 mls of growth media containing serum to neutralize the effect of the trypsin and transfer this solution to a conical vial before performing a cell count.

4.3 To get an average cell count, 10 μl of cells in media were added to a hemocytometer slide. This slide contains numerous grids that are used to help count cells. The cells located in the grids on each corner of the slide are counted, and the average number of cells in each grid is determined to be the number of cells per 10 μl and, by multiplying that number by 10,000, the number of cells per mL is determined. The total number of cells in a sample can be determined by multiplying the cells/mL by the number of mL in the sample. The concentration can be adjusted down by diluting the sample, using the following equation

$$C_{initial} \times V_{initial} = C_{desired} \times V_{desired.}$$

4.4 Based on cell count add media to the cell suspension to obtain the desired number of cells for the flask, plate, or slide, then add the correct amount of solution to each well/slide.

4.5 From the remaining solution, add 1mL of cell suspension to a new flask containing ~10-12mL media for re-growth, then return the flask to the incubator

4.6 Change media and reduce cell count every 2-4 days

5. NANOPARTICLE DOSING PROCEDURE:

5.1 Make nanoparticle dosing concentrations from stock concentrations of nanoparticles in water into fresh in DMEM/F12 media without serum. If you want to obtain images of these dosing solutions, use 15 mL conical tubes, small

clear plastic eppendorf tubes, or glass vials. Before dosing, mix the solutions well by vortexing and pipetting.

5.2 N2A cells are typically dosed 24 hours after seeding as described in Section 4 for passaging the cells. The existing growth media is aspirated prior to the addition of nanoparticle solutions.

5.3 Doses for nanoparticles are typically 0, 5, 10, 25, 50, 100 µg/ml. Doses for bulk materials are typically lower such as $AgNO_3$: 0, 0.5, 1, 2.5, 5, 10µg/ml or Mn acetate: 0, 1, 2.5, 5, 10, 25µg/ml. For 6-well plates, 1ml of dose per well, for 12 or 24-well plates, 0.5ml of dose per well. A typical 6-well plate set up is as follows:

0 (control)	Conc. 1	Conc. 2
Conc. 3	Conc. 4	Conc. 5

Perform assay in triplicate (3 plates each).

5.4 After dosing, label wells with dose and label plate with material used and the time, then return plates to incubator

5.5 Following 24 hours (or other time point eg. 12, 48 etc) assay plates for determined endpoint (MTS, LDH, etc)

6. MTS ASSAY OF VIABILITY

6.1 Following exposure interval, do NOT aspirate media. Add MTS stock directly to each well:

6 well plates = add 200 µl of MTS 5 mg/ml stock soln.

12 well plates = add 100-150 µl of MTS 5 mg/ml stock soln.

24 well plates = add 100 µl of MTS 5 mg/ml stock soln.

96 well plates = add 200 µl of MTS 5 mg/ml stock soln.

6.2 Incubate at 37° C in incubator until color develops (usually 30 minutes or may be longer)

6.3 Remove the MTS solution and lyse cells with 0.5 ml acidified isopropanol solution (acidified IPA) solution to well and place on a stir plate for approximately 30 minutes.

6.4 Remove the solutions and place into eppendorf tubes to vortex to obtain homogeneous staining of the formazan crystals

6.5 Centrifuge the purple solution at high speed to spin out nanoparticles.

6.6 Transfer 200 ul of samples into wells of 96 well plate in duplicate or greater

6.7 Read plates at 570 nm minus 630 nm on a microplate reader

6.8 For the Molecular Devices SpectraMax190, follow the instructions below: Start, Programs, Softmax 3.1, Spf (click), open old file, click template, highlight old data, clear, highlight cells, enter group name ie. control, what it is, sample 0, 25, etc. for concentrations Turn on microplate reader machine (needs a minute to calibrate), drawer will open, snap plate in place, click read, normal, ok, replace. Turn off microplate reader and log-out/turn off computer. Throw away materials into red trash can for biohazard.

6.9 MTS DATA ANALYSIS/RECORDS:

$CT = 100 * ((OD_t/OD_c)$

CT = % of MTS reducing activity

OD_t= Optical Density of treated samples

OD_c= Optical Density of control

7. IMAGING FOR NANOPARTICLE UPTAKE

7.1 After plating and dosing cells as described above, remove nanoparticles and wash 1-2X with PBS if necessary.

7.2 Remove the chambers from slide if necessary and mount with a coverslip, then seal edges with clear nail polish

7.3 Mount slide inverted onto microscope, then focus image.

7.4 Once your image is in focus through the microscope binocular lenses, start the QCapture program. Press the camera icon, then preview. To adjust the brightness of the image, change the exposure slide bars. After your preview image is adjusted for focus and brightness, make sure acquisition is set to 1x1, 8-bit B&W, or 24 bit RGB, then press snap to capture image. Go to File, Save as to save image. Do not use any symbols including periods in your file name and save original files as tif.

7.5 To add scale bars, press the micrometer icon and select the appropriate magnification. For 20x images, use 20 micron bar, for 60x images, use 100 micron bar. Right click to burn micron bar onto file.

8. QUALITY CONTROL

7.1 Use a positive and negative control, examine cells for viability *(ie.* Control with no nanoparticles and toxic material such as AgNO3 or CdO).

LIMITATIONS OF PROCEDURE:

8.1 This procedure can be slightly modified for non-adherent cells and cell-specific media should be used.

9. PROCEDURE NOTES: Too many or two few cells may skew the results of the MTS assay.

Appendix B – Basic N2A Cell Maintenance

1. Spray alcohol on gloves and on the work space area in the hood to avoid contamination!

2. Cells are observed under light microscope to see how healthy they look and whether they are becoming fairly confluent (getting crowded). If this is the case then it is time to split them or plate them.

3. Aspirate old media with the vacuum but be careful not to remove the cells that are adherent to the flask.

4. Add new GROWTH media (~5-10mL). This is the DMEM F12K Ham's + 1% pen/strep AND 10% FBS.

5. Scrape the bottom gently with a cell scrape to remove cells that are sticking to the bottom.

6. Mix the media around and then put all of the media along with the cells into a conical vial with the 10mL glass pipette. A 50mL conical vial usually works well for holding the media with the cells.

7. If cells are needed to plated at a certain density, the Nexcelom Bioscience's Cellometer Vision was used for automated cell counts. Dilutions can be easily calculated to plate at desired densities.

8. Add desired mL of cells into each container (flask, 96-well plate, chambered slides, etc). For 96-well plates, 200uL is added per well with a multi-chambered pipette. 1mL of cell solution is added per chamber. Leftover cell solution is divided into the T-75 flasks for continued growth. Cells can be diluted with extra growth media. If cells are

only split, extra cells can be discarded or put into another T-75 flask for growth9. For flasks, make sure to add enough growth media so that each one has ~10-15mL.

9. Be sure to observe the cells under the light microscope after they are put into the flasks. They will not have adhered to the bottom of the flasks yet so they will look rounder. Cells need to stay as healthy as possible for experiments. They will most likely need to be split about every 3 days. Beyond this they may become too confluent and thus less healthy.

10. Put everything back into the incubator and close the inner door securely.

12. Remember that the cells are can never exposed to the air unless they are in the hood. Be sure to cover the 96 well plate, screw the cap on the flasks, etc. All other pipettes and cell scrapers must all be opened in the hood.

Appendix C: Operating instructions for the LVEM (Schrand & Hussain, 2010).

PURPOSE/PRINCIPLE: This standard operating procedure describes methods for using the Low Voltage Electron Microscope (LVEM).

KEY WORDS: Nanoparticle agglomeration, Cell uptake

1. SAFETY AND OPERATING PRECAUTIONS:

1.1 Wear appropriate gloves when handling samples/sample holder.

1.2 Properly dispose of unused/spent toxic materials (nanoparticles).

2. EQUIPMENT/MATERIALS:

2.1 Cu TEM grids, preferably carbon-coated or uncoated

2.2 Nanoparticles in solution (typically water or ethanol)

4. PROCEDURE:

4. 1 Prepare samples on TEM grids by drop-casting solution with micropipetter onto Whatman's filter paper to remove excess solution (typically NP solution concentrations should be ~50 μg/ml for ease in finding NPs). Store in grid box until ready to image.

4.2 IP switch remains ON, do not turn this off.

4.3 Turn on the microscope (MIC) switch.

4.4 Turn on the camera (top of camera has its own switch)

4.5 Turn on turbo pumps (PS).

4.5 Open software on computer by double-clicking icon.

4.6 Log in with username and password: guest, guest on computer and sign in log book with Name, Date, Time, Initial ip1 and ip2 values.

4.7 Wait for vacuum pump LED to change from red/orange to GREEN

4.8 If sample holder left in LVEM, pull straight out---this is the preferred storage location for sample holder. You should see little nub on holder before pulling out. (if not please find Amanda for further instruction)

4.9 Insert TEM grid into holder with provided sample holder carrier by gently lifting Cu flap and replacing it with fine tweezers.

4.10 Re-insert sample holder into LVEM by pushing straight back. Turn airlock to GREEN tape (open). Wait for LED light to turn GREEN, then continue to insert sample by turning holder 45º clockwise and slowly pushing in (requires some force). Watch ip1 values (sample chamber ip current). **These must be in black before HV turned on** (Step 4.13)

4.11 Fasten silver knob until tight (do not over tighten), then press in black knob at the end of the sample holder.

4.12 Turn on electron gun (HV) on the black console and notice that small RED light comes on at the top of the sample chamber. WAIT ~ 15 minutes for gun emission to stabilize to 5.4 kV (Preset). With objective lenses out of the way of the YAG screen, you should be able to see a dot indicative of the electron beam. If not, adjust HV (~5.15kV) and move sample with joystick on black console until a dot is present in the center of the YAG screen.

4.13 Turn objective lens to 4x objective, then click VIEWS, CAMERA, START/STOP from software menu to view beam on the computer screen. Spread beam out by adjusting HV, gain (ie. 500). ***Make sure camera was turned on at the top of the LVEM and that the pull out knob on the side of the camera is all the way out.**

4.14 For an overview of the sample, select MODE, SCAN MODE. For TEM, change to MODE, TEM. To change magnification, use black knob on console. To adjust focus, use HV and Z height adjustment on sample stage as well as the YAG dial. ***It may be easier to start focusing on the edge of the grid.**

4.15 TO CHANGE/REMOVE SAMPLE: Turn off HV, unscrew silver knob, pull sample holder straight out, **CAREFUL HERE: turn sample holder 30º (you should see small silver knub in sample exchange area), close off valve (you should see orange tape),** LED should be GREEN, pull holder straight out, remove sample from sample holder and place in grid box for storage)

4.16 TO REINSERT NEW SAMPLE: Ensure that LED light is GREEN, then start at step 4.10 above. ***Make sure that LED light is GREEN, no HV**

is on (there is NO small red light on above sample chamber) before proceeding with sample insertion.

4.17 SHUT DOWN: Remove sample from holder as described in step 4.15 and place grid for storage in grid box. Push sample holder (without any sample in it) into sample chamber for storage, ***HV must be turned OFF, you should see orange tape indicating that vacuum valve is CLOSED, turn off MIC and PS, turn off camera at top of microscope, close software, touch computer screen for screen-saver mode.**

RECORDING IMAGES/SAVING FILES:

5.1 In the VIEWS, CAMERA, START/STOP, select CAPTURE IMAGE to take a final picture, then select where you want to save file in your user folder. Keep the magnification as part of the image if you want to calibrate for size measurements later on (See attachment on QCapture Pro Software to make measurements on image).

QUALITY CONTROL:

7.1 Check with Amanda on beam alignments when sample is removed for correct position/stigmatism.

LIMITATIONS OF PROCEDURE:

8.1 Very small nanoparticles, thick sections and coated grids may pose imaging problems in LVEM. No samples can be wet.

9. PROCEDURE NOTES:

10. REFERENCES:

11. ATTACHMENTS:

Attachment 1: About the LVEM System

Attachment 2: QCapture Pro Software for Measuring Images

ATTACHMENT 1: About the LVEM System

The LVEM5 electron microscope is designed for a broad range of applications in biology, medicine, and materials science, with most applications in the field of organic materials (polymers) and nanotechnology research.

The LVEM5 is a research tool for observation of objects composed of light elements (H, C, N, O, S, P) that can be observed with a high contrast without heavy-metal staining or shadowing. Samples composed of heavier elements can be observed as nanoparticles or ultra-thin films.

The high contrast of the light elements is achieved using significantly lower electron energy (5 keV) compared to standard transmission electron microscopes (TEM). Lowering the accelerating voltage from 100 kV to 5 kV significantly increases electron scattering, improving the contrast of the sample (e.g. more than 10-times greater contrast for thin carbon films).

ATTACHMENT 2: QCapture Pro 6.0 Software for Measuring Images

1. Turn on computer.
2. Switch camera on (black switch on top of camera).
2. Open the QCapture Pro 6.0 software.
4. File, open, desktop, user files, select folder/file and open
5. To measure, select measure on menu bar, calibration, calibration wizard, calibrate active image, LVEM_TEM mode_mag, nanometers, next, draw reference line, “1000” or other units to match current micron bar on image
6. Check your calibration with Calibration, select spatial, marker, move, right click to burn to image
7. To make measurements, select Measure, measure distances, measure the area on image, then under the Measure menu select snap measurements to burn them to image, then file save as (rename with _measured or other label to distinguish from original file).

Appendix D: Checklist for the Transmission Electron Microscope – CM 200 Lab 6
Provided by Dr. Robert Wheeler, modified by Capt S. V. Brownheim

The TEM at Lab 6 at the Materials Lab is a 200 kV TEM

1. Make sure panel lights are on – two LEDs should be on: UHV and HVAC
2. Check the system vacuum, make sure IGP < 20, P3 < 70
3. High Tension (HT) = 200 kV?
4. LN2 – Liquid nitrogen should be filled in the canister and coils remain cooled
5. Load TEM specimen with correct tools onto appropriate sample holder, check for dust particles on O-ring and clean as necessary
6. Load TEM sample holder along with specimen in the following way:
    a. Check vacuum again
    b. Start inserting sample with the small pin pointed in the 3 o-clock position while inserting the rod as straight as possible
    c. A "catch" should be felt and the vacuum pump should start pumping, the red light should turn on near the sample holder
    d. Spin from the 3 o-clock position to the 5 o-clock position and gently put the sample holder into the recess
    e. Select the correct holder on the screen, connect the plug, and press "ready"
    f. When the vacuum stops pumping the red light should go out
    g. Starting "opening" the sample, waiting for IGP to jump and then stabilize
    h. Wait for equilibration, then completely open and feed the sample holder the rest of the way in until secured
    i. Specimen is now loaded
7. C2 Aperture - using the top aperture to adjust and center the maximum illumination from the electron beam possible
8. Eucentric Height (Objective Lens should equal 5480) – adjust by using "step" size knobs
9. Gun Tilt – make the illumination as bright as possible
10. Gun Shift
11. Pivot Points
12. Rotation Alignment – press the "ROT CENTER" button to optimize image and make the image move the least amount possible

*The image on the next page shows the control panels on the TEM

Left Hand Panel

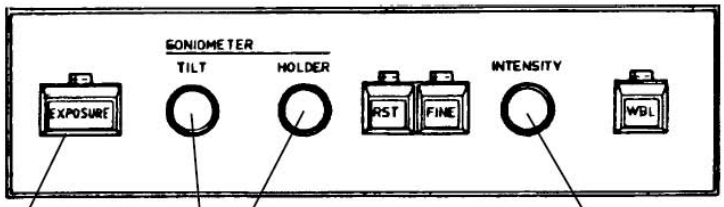

Expose Image

A - B Tilts

Beam Intensity

Right Hand Panel

HT=200kV
(Parameters)

Objective Lens Value
(Parameters-Display Currents)

Filament
(Modes-Configuration)

Vacuum

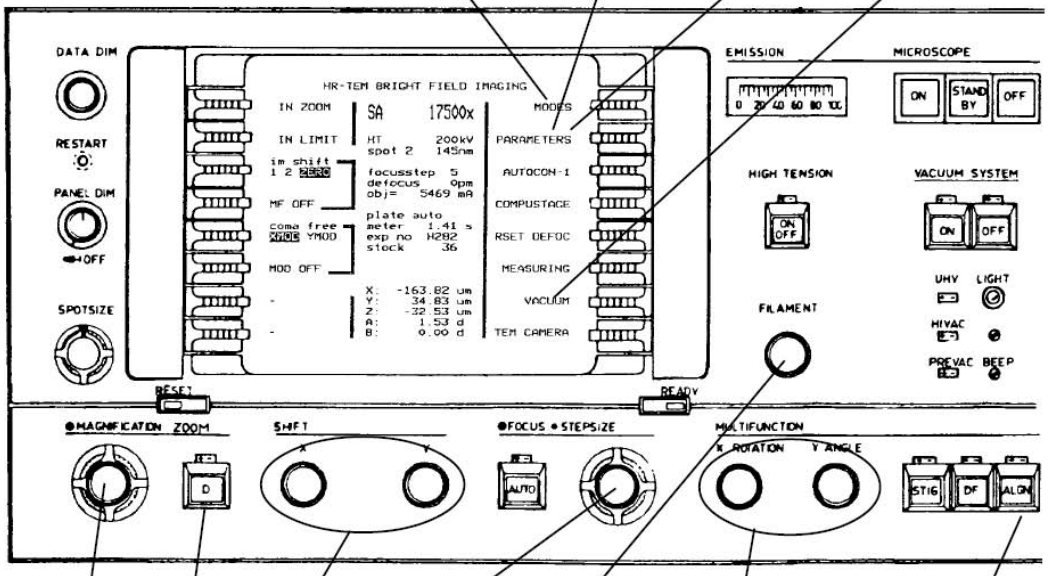

Magnification

Diffraction Mode

Beam Shifting

Focus

Filament

Adjust Alignments

Gun Tilt
Gun Shift
Pivot Points
Rotation Alignment

Appendix E: Cell Sample Preparation for the Scanning Electron Microscope (Schrand, 2006).

1. Allow sufficient time to start and complete protocol. Typically, the fixation and dehydration take half of a day and then the cells are left overnight. The next day, drying, mounting, coating, and imaging would require an additional 3 or more hours.

2. Grow cells on Aclar polymer discs or other surface in multi-well dishes according to standard cell culture techniques.

3. Remove growth medium and wash 2X each for 10 minutes with PBS.

4. Add glutaraldehyde/Na cacodylate solution (2.5% glut/form in 0.1M Na caco pH 7.4) at 4 °C for 1 hour to fix.

5. Remove fixative and wash 3X each for 15 minutes with 0.1 M Na caco buffer, pH 7.4 (dilute 0.2M in half with double distilled deionized water).

6. Remove buffer and start dehydration series (50, 70, 90, 100, 100, 100, 100%) in ethanol for 15 minutes each, then leave in fresh 100% ethanol overnight in a closed dish to prevent evaporation.

7. Transfer cells in multiwell plates in 100% ethanol to the NEST at UD.

8. Critical Point dry and mount to SEM stub with double-sided carbon tape.

9. Coat with gold in sputter coater.

10. Image in High Resolution SEM (make sure that you have been properly trained or a staff person is available to assist you on the instrument. Once you are trained, the time can be scheduled online at www.nestlaboratory.com before showing up for your session).

Appendix F: Operating Instructions for Malvern's Zetasizer for Dynamic Light Scattering (DLS)

1. Log on to DLS computer.
2. Open Zetasizer software and click on "manual measurement", ensuring proper settings are set and select the correct sample holder. For zeta potential measurements the clear zeta cuvette must be selected. Select either "size" or "zeta potential" to run with.
3. Vortex sample.
4. Close cuvette with the appropriate tops and insert into cuvette holder.
5. Click the measure button.
6. Measurement records are saved automatically in the main record area under the file name. Data can be exported to Microsoft Excel or Microsoft Word.

Appendix G: Hyperspectral Imaging

Olympus IX71 Inverted Fluorescent Microscope with CytoViva 150 attachment and 12 bit QICAM from IMAGINE (Lab 160)

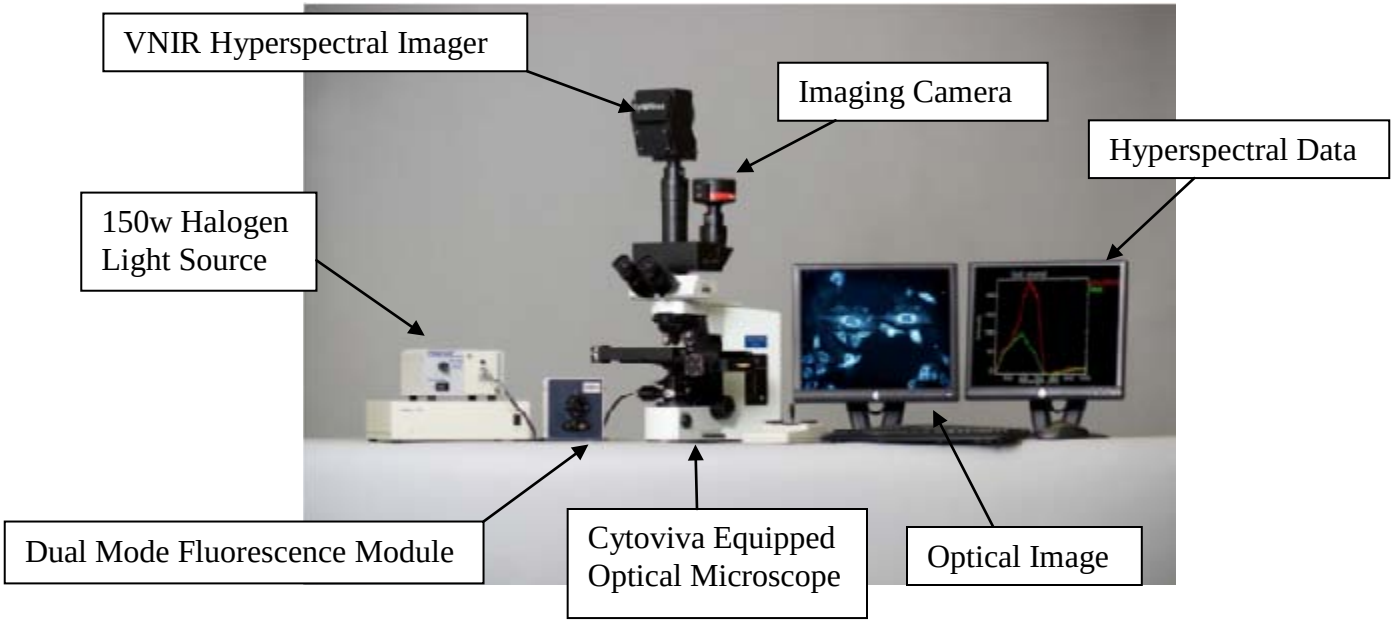

HSI system set up, picture from the manufacturer (Cytoviva, 2011). http://www.cytoviva.com/product_hyperspectral_imaging.htm

1. Samples of the N2A cells or particles are dropped onto glass slides. Cells are covered with a glass cover-slip and sealed around the edges with nail polish. Care is taken to ensure there's not too much cell solution on the glass slide. Particles at the desired concentration are dropped onto the glass slides and allowed to dry under the hood. Glass cover-slips are added and the edges are sealed with nail polish.

2. Once the sample slides are prepared the HSI system was used to capture the images of the samples and appropriate spectra are captured.

Bibliography

Agency for Toxic Substances and Disease Registry, "Toxicological Profiles for Copper". Sept, 2004 http://www.atsdr.cdc.gov/ToxProfiles/tp.asp?id=206&tid=37

American Type Culture Collection (ATCC), "Production Description for CCL-131, Neuro-2a". 10 Oct, 2010 http://www.atcc.org/ATCCAdvancedCatalogSearch/ProductDetails/tabid/452/Default.aspx?ATCCNum=CCL-131&Template=cellBiology

Chen, Z., Meng, H., Xing G., Chen, C., Zhao, Y., Jia G., Wang T., Yuan H., Ye C., Zhao, F., Chai Z., Zhu, C., Fang, X., Ma, B., Wan, L., "Acute toxicological effects of copper nanoparticles in vivo" *Toxicology Letters* 163: 109-120 (2006).

Cioffi, N., Torsi L., Ditaranto N., Tantillo, G., Ghibelli, L., Sabbatini L., Belve-Zacheo T., D'Alessio M., Zambonin P.G., Traversa E., "Copper Nanoparticle/Polymer Composites with Antifungal and Bacteriostatic Properties" *Chem. Mater.* 17: 5255-5262 (2005).

Committee to Review the National Nanotechnology Initiative, National Research Council, "A Matter of Size: Triennial Review of the National Nanotechnology Initiative". 12 January 2011 http://www.nap.edu/catalog/11752.html

Cytoviva, "The Cytoviva Hyperspectral Imaging System". 4 Jan 2011 http://www.cytoviva.com/product_hyperspectral_imaging.htm

Department of Energy, Offices of Basic Energy Sciences (BES), "Scale of Things" 5 Jan 2011 http://www.science.doe.gov/bes/scale_of_things.html

Dingman, S., "Nanomaterials in Organic Photovoltaic Devices", Sigma-Aldrich.com *ChemFiles* 5: 4 (2005).

EPA, Control of Nanoscale Materials under the Toxic Substances Control Act. 1 January 2011 http://www.epa.gov/oppt/nano/

Ganesh, R., Smeraldi, J., Hosseini, T., Khatib, L., Olson, B.H., Rosso, D., "Evaluation of Nanocopper Removal and Toxicity in Municipal Wastewaters" *American Chemical Society* 3: 20 (2010).

Goodman, M.T., Gurney, J.G., Smith, M.A., Olshan, A.F., "Sympathetic Nervous System Tumors" National Cancer Institute, National Cancer Institute, Surveillence Epidemiology and End Results, 10 Jan, 2011 http://seer.cancer.gov/publications/childhood/sympathetic.pdf

Grocholl, L., "Coatings", Sigma-Aldrich.com *ChemFiles* 5: 5 (2005a).

Grocholl, L., "Antibacterial Applications", Sigma-Aldrich.com *ChemFiles* 5: 7 (2005b).

Guo, K., Pan, Q., Wang, L., Fang, S., "Nano-scale copper-coated graphite as anode material for lithium-ion batteries" *J. Appl. Electrochem.* 32: 679-685 (2002).

Howard, J., "Strategic Plan for NIOSH Nanotechnology Research Filling the Knowledge Gaps". Nanotechnology Research Program National Institute for Occupational Safety and Health Centers for Disease Control and Prevention (2005).

Kotov, N., "Nanotube-Polymer Composites for Ultra Strong Materials", Sigma-Aldrich.com *ChemFiles* 5: 9 (2005).

Liu, G., Li., X., Qin, B., Xing, D., Guo, Y., Fan, R., "Investigation of the mending effect And mechanism of copper nanoparticles on a tribologically stressed surface" *Tribology Lett* 17 (4): 961-966 (2004).

Lonza Pharamaceuticals, "Penicillin-Streptomycin". 2 Jan 2011. http://www.biocenter.hu/pdf/penstrep.pdf

Lvov, Y., "Layer-by-Layer Nanoassembly for Drug Delivery", Sigma-Aldrich.com *ChemFiles* 5: 7 (2005).

Macia, E., Ehrlich, M., Massol, R., Boucrot, E., Brunner C., Kirchhausen T., "Dynasore, a cell-permeable inhibitor of dynamin" *Dev Cell* 6: 839-50 (2006).

Malvern Industries, "Zetasizer Nano User Manual" 6 June, 2010. http://www.malvern.com/

Midander, K., Cronholm, P., Karlsson, H.L., Elihn, K., Möller, L., Leygraf C., Wallinder, I.O., "Surface Characteristics, Copper Release, and Toxicity of Nano- and Micrometer-Sized Copper and Copper(II) Oxide Particles: A Cross-Discipinary Study", *Small*, 5, No. 3: 389-399 (2009).

Miller M.M., Lazarides, A.A., "Sensitivity of Metal nanoparticle Surface Plasmon Resonance to the Dielectric Environment", *J. Phys. Chem. B*, 109: 21556-21565 (2005).

Minteer, S. D., "Nanomaterials in Fuel Cells", Sigma-Aldrich.com *ChemFiles* 5: 8 (2005).

Murdock, R.C., Braydich-Stolle, L., Schrand, A.M., Schlager, J.J., Hussain, S.M. "Characterization of Nanomaterial Dispersion in Solution Prior to *In Vitro* Exposure Using Dynamic Light Scattering Technique" *Toxicological Sciences* 101:239-253 (2008).

Murthy, R.C., Lal S., Saxena D.K., "Effect of manganese and copper interaction on behavior and biogenic amines in rats fed a 10% casein diet", *Chem Biol Interact* 37: 299-308 (1981).

Nexcelom Biosciences, "Cellometer Vision". 25 Jan 2011. http://www.nexcelom.com/Cellometer-Vision/Vision-How-it-Works.html

NIOSH "*Strategic Plan for NIOSH Nanotechnology Research and Guidance: Filling the Knowledge Gaps"* (Nov, 2009).

Nordberg, G.F., Fowler, B.A., Nordberg, M., Friberg, L., "Handbook on the Toxicology of Metals, Third Edition", Academic Press (2007).

Oberdörster, G., Maynard, A., Donaldson, V., Castranova, J., Fitzpatrick, K., Ausman, J., Carter, J., Karn, B., Kreyling, W., Lai, D., Olin, S., Monteiro-Riviere, N., Warheit, D., Yang, H., "Principles of characterizing the potential human health effects from exposure to nanomaterials: elements of a screening strategy" *Part. Fibre Toxicol* 2 (2005a).

Oberdörster, G., Oberdörster, E., Oberdörster, J., "Nanotoxicology: An Emerging Discipline Evolving from Studies of Ultrafine Particles" *Environmental Health Perspectives* 113: 7 (2005b).

Promega, "Instructions For Use: Cell Titer 96® Aqueous Non-Radioactive Cell Proliferation Assay" (2009).

PubMed Health, National Center for Biotechnology Information, "Neuroblastoma" 8 Jan 2011. http://www.ncbi.nlm.nih.gov/pubmedhealth/PMH0002381

Rohatgi, P., Schultz, B., Ferguson, J.B., "Metal Matrix Nanocomposites for Structural Applications", Sigma-Aldrich.com *ChemFiles* 5: 10 (2005).

Schrand, A.M., Hussain, S.M., "Nano-materials in Biotechnology Applications" In Progress (2010).

Shapira, P., Wang, J., "Follow the Money" *Nature* 468 (2010).

Schrand, A.M., Rahman, M.F., Hussain, S.M., Schlager, J.J., Smith, D.A., Syed A.F., "Metal-based nanoparticles and their toxicity assessment" *John Wiley & Sons, Inc* 2 (2010).

Schrand, A.M., Unpublished Data In Preparation (2011).

Shaffner, J., Van Veld, R.D., "Charging effects in the Scanning Electron Microscope" *J. Phys. E: Sci. Instrum* 4:633 (1971).

Sigma-Aldrich, "Dulbecco's Modified Eagle's Medium Nutrient Mixture F-12 Ham" 8 Aug 2010. http://www.sigmaaldrich.com/catalog/ProductDetail.do?lang=en&N4=D2906|SIGMA&N5=SEARCH_CONCAT_PNO|BRAND_KEY&F=SPEC

Sigma-Aldrich, "Fetal Bovine Serum". 9 Dec 2010. http://www.sigmaaldrich.com/life-science/cell-culture/cell-culture-products.html?TablePage=9628642

Strano, M., Baik, S., Barone, P., "Carbon Nanotube-Based Biosensors", Sigma-Aldrich.com *ChemFiles* 5: 6 (2005).

Tocris Bioscience, "Dynasore". 7 August 2010. http://www.tocris.com/dispprod.php?ItemId=122658

Yguerabide, J., Yguerabide, E.E., "Light-Scattering Submicroscopic Particles as Highly Fluorescent Analogs and Their Uses as Tracer Labels in Clinical and Biological Applications", *Analytical Biochemistry*, 262: 137-156 (1998).

REPORT DOCUMENTATION PAGE

Form Approved
OMB No. 074-0188

1. REPORT DATE *(DD-MM-YYYY)*	**2. REPORT TYPE**	**3. DATES COVERED** *(From – To)*
24-03-2011	Master's Thesis	May 2010 – Mar 2011

4. TITLE AND SUBTITLE
Characterization and *in vitro* toxicity of Copper Nanoparticles (Cu-NPs) in murine neuroblastoma (N2A) cells

5a. CONTRACT NUMBER

5b. GRANT NUMBER

5c. PROGRAM ELEMENT NUMBER

6. AUTHOR(S)
Brownheim, Sitao, V., Capt, USAF, BSC

5d. PROJECT NUMBER
None

5e. TASK NUMBER

5f. WORK UNIT NUMBER

7. PERFORMING ORGANIZATION NAMES(S) AND ADDRESS(S)

Air Force Institute of Technology
Graduate School of Engineering and Management (AFIT/EN)
2950 Hobson Way
WPAFB OH 45433-7765

8. PERFORMING ORGANIZATION REPORT NUMBER
AFIT/GES/ENV/11-M01

9. SPONSORING/MONITORING AGENCY NAME(S) AND ADDRESS(ES)
USAF School of Aerospace Medicine Occupational and Environmental Health (Force Development Division)
1050 Forrer Blvd
Kettering OH 45420
(937) 656-8286 DSN (986-8286) Attn: Maj Robert Eninger
Robert.Eninger@wpafb.af.mil

10. SPONSOR/MONITOR'S ACRONYM(S)
USAFSAM/OED

11. SPONSOR/MONITOR'S REPORT NUMBER

12. DISTRIBUTION/AVAILABILITY STATEMENT
APPROVED FOR PUBLIC RELEASE; DISTRIBUTION UNLIMITED

13. SUPPLEMENTARY NOTES
This material is declared a work of the United States Government and is not subject to copyright protection in the United States

14. ABSTRACT

Nanomaterials, classified as materials within the 1 - 100 nanometer range, have seemingly endless applications. It is very important to the Air Force to increase the understanding of Cu-NPs and the possible health impacts from nanomaterial exposure prior to wide-spread industry and military use. Therefore, the purpose of this research is to thoroughly characterize the properties of three different copper samples upon suspension into aqueous solutions over time: Cu-NPs (Cu 25 nm), CuO-NPs (CuO 40 nm), and Cu-MSP (Cu 500nm). Additionally, this research seeks to observe *in vitro* effects upon murine neuroblastoma cells (N2A) by these three types of particles as well as by $CuCl_2$. Microscopy techniques indicate observable changes in oxidation for Cu-NP 25 nm and CuO-NP 40 nm after suspension in water over long incubation. In general, agglomerations of the particles increase when dosed with the endocytosis inhibitor Dynasore. In terms of cellular viability, $CuCl_2$ is the least toxic at all concentrations. Cu-NP 25 nm is less toxic at low concentrations (< 25 µg/mL) than Cu-MSP 500 nm and CuO-NP 40 nm. At concentrations above 25 µg/mL, Cu-NP 25 nm becomes comparable in toxicity to CuO-NP 40 nm and more toxic than Cu-MSP 500 nm.

15. SUBJECT TERMS
Copper nanoparticles, Characterization, *in vitro* effects, Murine neuroblastoma cells (N2A), Cu-NPs (Cu 25 nm), CuO-NPs (CuO 40 nm), and Cu-MSP (Cu 500nm), Dynasore, Microscopy, cellular viability

16. SECURITY CLASSIFICATION OF:			**17. LIMITATION OF ABSTRACT**	**18. NUMBER OF PAGES**	**19a. NAME OF RESPONSIBLE PERSON**
a. REPORT	**b. ABSTRACT**	**c. THIS PAGE**			Dr. Charles A. Bleckmann (AFIT/ENV)
U	U	U	UU	120	**19b. TELEPHONE NUMBER** *(Include area code)* 937-255-3636 ext. 4721

Standard Form 298 (Rev. 8-98)
Prescribed by ANSI Std. Z39-18

Form Approved
OMB No. 074-0188